EC
Journals.ASM.org

Secretion of Polypeptide Crystals from *Tetrahymena thermophila* Secretory Organelles (Mucocysts) Depends on Processing by a Cysteine Cathepsin, Cth4p

Santosh Kumar, Joseph S. Briguglio,* Aaron P. Turkewitz

Department of Molecular Genetics and Cell Biology, The University of Chicago, Chicago, Illinois, USA

In many organisms, sophisticated mechanisms facilitate release of peptides in response to extracellular stimuli. In the ciliate *Tetrahymena thermophila*, efficient peptide secretion depends on specialized vesicles called mucocysts that contain dense crystalline cores that expand rapidly during exocytosis. Core assembly depends of endoproteolytic cleavage of mucocyst proproteins by an aspartyl protease, cathepsin 3 (*CTH3*). Here, we show that a second enzyme identified by expression profiling, Cth4p, is also required for processing of proGrl proteins and for assembly of functional mucocysts. Cth4p is a cysteine cathepsin that localizes partially to endolysosomal structures and appears to act downstream of, and may be activated by, Cth3p. Disruption of *CTH4* results in cells (Δ*cth4*) that show aberrant trimming of Grl proproteins, as well as grossly aberrant mucocyst exocytosis. Surprisingly, Δ*cth4* cells succeed in assembling crystalline mucocyst cores. However, those cores do not undergo normal directional expansion during exocytosis, and they thus fail to efficiently extrude from the cells. We could phenocopy the Δ*cth4* defects by mutating conserved catalytic residues, indicating that the *in vivo* function of Cth4p is enzymatic. Our results indicate that as for canonical proteins packaged in animal secretory granules, the maturation of mucocyst proproteins involves sequential processing steps. The Δ*cth4* defects uncouple, in an unanticipated way, the assembly of mucocyst cores and their subsequent expansion and thereby reveal a previously unsuspected aspect of polypeptide secretion in ciliates.

Regulated secretion of peptides from intracellular stores plays many key roles in intercellular communication and tissue coordination in animals (1). A highly specialized organelle in neuroendocrine cells, the secretory granule, is required for peptide generation, storage, and release (2). The bioactive peptides are generated during secretory granule formation by the action of proteolytic enzymes on polypeptide precursors (3). Proteolytic processing occurs in a post-*trans*-Golgi network (TGN) compartment, the immature granule, to which propeptides are sorted away from bulk protein traffic, and is a multistep process involving several classes of enzymes (4–6). The best studied among these are a family of serine proteases called prohormone convertases (7). Related to bacterial subtilisins, prohormone convertases (PCs) catalyze endoproteolytic cleavage at defined motifs in their substrates. The products of that cleavage can then undergo trimming, for which one important factor is carboxypeptidase E (CPE) (8). Defects in both PCs and CPE are linked with disease (9, 10).

Signaling via peptide secretion appears to be widespread in eukaryotes and has also been well documented for fungi, amoebozoa, and plants(11–13). In the oligohymenophorean ciliates *Tetrahymena thermophila* and *Paramecium tetraurelia*, regulated peptide secretion occurs from organelles that share striking similarities with secretory granules in animals (14, 15), although they may be more closely related to lysosomes (16). Called mucocysts in *Tetrahymena* and trichocysts in *Paramecium*, these organelles serve to concentrate a subset of newly synthesized proteins in the secretory pathway and to store them in the form of elaborate protein crystals until their release is triggered by extracellular stimuli (17). Such stimuli provoke mobilization of extracytosolic calcium, which promotes exocytic membrane fusion (18, 19). During exocytosis, the secretory proteins are rapidly extruded, due to the fact that the crystalline lattices expand rapidly and directionally. Thus, the function of secretory organelles in ciliates depends upon the assembly of protein crystals that can undergo spring-like elongation (20, 21).

The most abundant proteins stored in and released from *Tetrahymena* mucocysts belong to two families, called GRT (for granule tip) and GRL (for granule lattice) (22, 23). Studies of the Grl proteins, and the related *P. tetraurelia* tmp proteins, have demonstrated that extensive proteolytic processing occurs during mucocyst and trichocyst synthesis (20, 24–26). Processing is essential to generate the crystal-ordered luminal core, whose formation can therefore be thought of as the product of a morphogenetic program (26). The enzymes involved, however, and the precise roles of processing in core assembly have in general only been inferred. Recently, we reported that an aspartyl cathepsin, Cth3p, plays an essential role, since disruption of the *CTH3* gene resulted in cells (Δ*cth3*) that completely failed to process Grl proproteins and, consequently, to assemble crystalline mucocyst cores (27). *CTH3*

Received 27 March 2015 **Accepted** 10 June 2015

Accepted manuscript posted online 19 June 2015

Citation Kumar S, Briguglio JS, Turkewitz AP. 2015. Secretion of polypeptide crystals from *Tetrahymena thermophila* secretory organelles (mucocysts) depends on processing by a cysteine cathepsin, Cth4p. Eukaryot Cell 14:817–833. doi:10.1128/EC.00058-15.

Address correspondence to Aaron P. Turkewitz, apturkew@midway.uchicago.edu.

* Present address: Joseph S. Briguglio, Department of Neuroscience, University of Wisconsin, Madison, Wisconsin, USA.

This article is dedicated to our late colleague, friend, and mentor, Don Steiner, a pioneer in the field of proprotein processing.

Supplemental material for this article may be found at http://dx.doi.org/10.1128/EC.00058-15.

doi:10.1128/EC.00058-15

TABLE 1 Description of *Tetrahymena* strains

Strain name	Phenotype	Details of relevant genetic modification	Source
B2086	Wild type for exocytosis	None	J. Gaertig (University of Georgia, Athens, GA)
CU428	Wild type for exocytosis	None	P. Bruns (Cornell University, Ithaca, NY)
UC810	Δ*cth4*; no detectable *CTH4* expression	Replaces nucleotides −50 to 925 of macronuclear *CTH4* ORF with NEO4 cassette	This study
Unstable cell line	High-level inducible expression of CFP-tagged Cth4p (cth4-1)	C-terminal fusion of Cth4p and CFP, expressed under the control of the *MTT1* promoter, on the multicopy rDNA[a] minichromosome	This study
UC811	Endogenous-level expression of GFP-tagged Cth4p (cth4-2)	C-terminal fusion of Cth4p and GFP, integrated at the macronuclear *CTH4* locus	This study
UC812	Endogenous-level expression of enzymatically disabled, GFP-tagged Cth4p (cth4-3)	Mutated variant of Cth4p (Cys^{352}→Ala; His^{505}→Ala), C-terminally fused to GFP, integrated at the macronuclear *CTH4* locus	This study
UC813	Inducible expression of His-tagged Cth4p (cth4p-6×His)	C-terminal fusion of Cth4p and 6His, expressed under the control of the *MTT1* promoter, at the macronuclear *MTT1* locus of CU428	This study
UC814	Inducible expression of His-tagged Cth4p (cth4p-6×His)	C-terminal fusion of Cth4p and 6His, expressed under the control of the *MTT1* promoter, at the macronuclear *MTT1* locus of Δ*cth3* (UC803)	This study

[a] rDNA, ribosomal DNA.

was originally identified as a candidate based on expression profiling, which is a powerful approach in this organism thanks to rich databases for gene expression (28–32).

Here, we show that a second enzyme identified by expression profiling, Cth4p, is also required for processing of proGrl proteins and for assembly of functional mucocysts. Cth4p is a cysteine cathepsin that localizes to endolysosomal structures and appears to act downstream of Cth3p. Disruption of *CTH4* results in cells (Δ*cth4*) that show aberrant processing of Grl proproteins, though such processing is clearly distinct from the processing defects in Δ*cth3* cells. Analysis of the processing intermediates that accumulate in Δ*cth4* mucocysts reveals a previously unsuspected major role for amino-terminal trimming at multiple sites within proGrl proteins during mucocyst biogenesis. Surprisingly, Δ*cth4* cells succeed in assembling crystalline mucocyst cores. However, those cores do not undergo normal directional expansion and thus fail to efficiently extrude from the cells, which therefore demonstrate grossly aberrant regulated exocytosis.

MATERIALS AND METHODS

Cell culture. Wild-type *T. thermophila* strains CU428.1 and B2086 were cultured in SPP medium (1% proteose peptone 0.2% dextrose, 0.1% yeast extract, 0.003% ferric EDTA). Experimental cultures were grown at 30°C with shaking at 100 rpm to 2×10^5 to 4×10^5 cells/ml unless otherwise indicated. Culture densities were determined using a Z1 Coulter Counter (Beckman Coulter Inc., Indianapolis, IN). All reagents were from Sigma-Aldrich Chemical Co. unless otherwise indicated. Details of *T. thermophila* strains are in Table 1. Strains described as wild type in the text refer to CU428.1, which is wild type with respect to mucocyst exocytosis.

Gene expression profiling and *in silico* analyses. Expression profiles were derived from the *Tetrahymena* Functional Genomics Database (http://tfgd.ihb.ac.cn/); for graphing, each profile was normalized to that gene's maximum expression level. Alignment of protein sequences was done using ClustalX (1.8) with default parameters.

Phylogenetic tree construction. Using protein BLAST (blastp), the *T. thermophila CTH4* and *CTH3* genes were used to identify potential homologs in ciliates, apicomplexans, *Arabidopsis*, and *Homo sapiens*, listed in Table S2 in the supplemental material. For tree building, the top hits were selected from each lineage, assembled, and aligned with ClustalX (1.8), and maximum-likelihood trees were constructed with MEGA5 (Molecular Evolutionary Genetics Analysis [http://www.megasoftware.net/]). Gapped regions were excluded in a complete manner, and percentage bootstrap values were derived from 1,000 replicates.

Expression of cathepsin 4 (*CTH4*) gene fusions. The Gateway (Invitrogen, Grand Island, NY) system was used to engineer cyan fluorescent protein (CFP) tagged-*CTH4* (TTHERM_00445920). The cloning strategy and expression conditions were identical to those used for *CTH3* (27).

Generation of cathepsin 4 knockout strains. The *CTH4* upstream region was amplified (1,688 bp), together with a portion of the open reading frame (ORF) plus downstream flank (1,793 bp total), which were subsequently subcloned into the SacI and XhoI sites of the neo4 cassette, respectively, using in-fusion cloning (Clontech, Mountain View, CA). The construct resulted in deletion of *CTH4* genic region from −50 to 925. The sequences of the primers are listed in Table S1 in the supplemental material. To assess the gene disruption, total RNA was isolated using RNeasy minikits as per the manufacturer's instructions (Qiagen, Valencia, CA). Forward and reverse primers used for *CTH4* are given in Table S1 in the supplemental material. The presence of the *CTH4* transcripts was assayed by one-step reverse transcription-PCR (RT-PCR) (Qiagen, Valencia, CA).

Biolistic transformations. The knockout vector was linearized by digestion with KpnI and SapI and transformed into CU428.1 cells by biolistic transformation (33).

Expression of Cth4p-green fluorescent protein (Cth4p-GFP) at the endogenous locus. *CTH4* (TTHERM_00445920) and 817 bp of *CTH4* downstream genomic sequence were amplified and cloned into the BamHI and HindIII sites of pmEGFP-neo4, respectively, by in-fusion cloning. To generate enzymatically disabled Cth4p, we used pCTH4-mEGFP-neo4 vector as the substrate. We generated Cys^{352}→Ala and His^{505}→Ala mutations, in which selected TGC (Cys) and CAC (His) codons in *CTH4* were replaced by GCA (Ala) and GCT (Ala), respectively, using the GeneArt site-directed mutagenesis PLUS kit (Invitrogen, Grand Island, NY). Final constructs were confirmed by DNA sequencing.

Expression of Cth4p-6×His. *CTH4*, without the stop codon, was amplified using a forward primer containing a PmeI restriction site and a reverse primer containing the coding sequence for 6×His, followed by a stop codon and an ApaI restriction enzyme site. The amplified product

was cloned into the pNCVB vector as described previously (27). The construct was linearized by digestion with SfiI and transformed into CU428.1 and Δ*cth3* cells by biolistic transformation, and transformants selected using 60 μg/ml of blasticidin and 1 μg/ml of $CdCl_2$. To induce transgene expression in growth or starvation media, cells were incubated for 2 h in 1 μg/ml of $CdCl_2$ (for SPP medium) or 0.1 μg/ml of $CdCl_2$ (for 10 mM Tris [pH 7.4]).

Live-cell microscopy. Live-cell imaging of cells expressing GFP-tagged fusion proteins was performed as described recently (27). Cth4p-GFP cultures were analyzed at 3×10^5 cells/ml unless otherwise indicated. Simultaneous imaging of Cth3-GFP with Lysotracker (Invitrogen) or FM4-64 (Life Technologies, CA) was performed as recently described (27).

Electron microscopy. Cells were grown overnight to stationary phase (10^6/ml), washed, fixed in 2% glutaraldehyde, 1% sucrose, and 1% osmium at 25°C in 0.1 M sodium cacodylate buffer, and section stained with uranyl acetate and lead citrate after embedding. Thin sections were viewed on a Tecnai G2 F30 Super Twin microscope (FEI).

Dibucaine and alcian blue stimulation. Dibucaine and alcian blue stimulation of exocytosis was performed as described previously (27, 34). Importantly, cells were washed and suspended in fresh medium immediately prior to stimulation. To assess secretion following dibucaine stimulation, 2 ml of the cell-free supernatants following low-speed centrifugation were carefully withdrawn and precipitated with 10% trichloroacetic acid (TCA). To remove flocculent, the remaining supernatant was aspirated, and the tube was cut with a razor just above the flocculent layer. Flocculent was then removed using a wide-mouth 200-μl pipette tip.

Flow cytometry. Detergent-permeabilized and antibody-stained cells were analyzed by FACS (BD FACSCalibur), as described previously (35).

Immunofluorescence. To visualize mucocysts or mucocyst intermediates, cells were fixed, permeabilized with detergent, immunolabeled with monoclonal antibody (MAb) 5E9 or MAb 4D11, and analyzed as described previously (27). For simultaneous imaging of Cth4p-CFP/GFP and mucocyst core proteins, cells were double stained with mouse MAb 5E9 and rabbit anti-GFP (27). Cells were imaged using a Leica SP5 II confocal microscope, and image data were analyzed as previously described (27).

SDS-PAGE and Western blotting. Whole-cell lysates and Western blots were prepared as described previously (27). GFP-tagged fusion proteins were immunoprecipitated from detergent lysates using polyclonal rabbit anti-GFP antiserum as described previously (16).

Isolation of secreted mucocyst contents for mass spectrometry. After dibucaine stimulation, 45 ml of cells at 10^6/ml was pelleted (15 ml/tube) for 2 min at top speed (2,000 × *g*) in a clinical centrifuge. All subsequent steps were at 4°C. After the supernatant was aspirated, the tubes were cut with a razor just about the flocculent layer, and the top of the flocculent layers were collected using a wide-mouthed transfer pipette and transferred to 1.5-ml conical tubes. Flocculent was then diluted 10-fold with 10 mM Tris (pH 7.4) and pelleted at 5,000 × *g* for 5 min, to extract small pellets of cells that were trapped in the flocculent. The flocculent samples were checked by light microscopy for cellular contamination, and dilution and repelleting was repeated 5 or 6 times until no cells were visible. The final samples were dissolved in 2× SDS-PAGE sample buffer, incubated for 15 min at 90°C, and then centrifuged (18,000 × *g*, 20 min, 4°C). The small solid pellets were discarded and the supernatants resolved by 4 to 20% SDS-PAGE, following by staining with Coomassie brilliant blue.

Mass spectrometry: trypsin digestion. The gel sections were chopped into ~1-mm^3 pieces, washed in distilled water (dH_2O), and destained using 100 mM NH_4HCO_3 (pH 7.5) in 50% acetonitrile. Reduction was performed by addition of 100 μl of 50 mM NH_4HCO_3 (pH 7.5) and 10 μl of 200 mM tris(2-carboxyethyl)phosphine HCl at 37°C for 30 min. The proteins were alkylated by addition of 100 μl of 50 mM iodoacetamide prepared fresh in 50 mM NH_4HCO_3 (pH 7.5) and allowed to react in the dark at 20°C for 30 min. Gel sections were washed in water and then acetonitrile and vacuum dried. Trypsin digestion was carried out overnight at 37°C with a 1:50 to 1:100 enzyme-protein ratio of sequencing grade-modified trypsin (Promega) in 50 mM NH_4HCO_3 (pH 7.5) and 20 mM $CaCl_2$. Peptides were extracted with 5% formic acid and vacuum dried.

HPLC for mass spectrometry. Samples were resuspended in high-performance liquid chromatography (HPLC)-grade water containing 0.2% formic acid (Fluka), 0.1% trifluoroacetic acid (TFA; Pierce), and 0.002% Zwittergent 3-16 (Calbiochem), a sulfobetaine detergent. The peptide samples were loaded onto a 0.25-μl C_8 OptiPak trapping cartridge custom-packed with Michrom Magic (Optimize Technologies) C8, washed, then switched in-line with a 20-cm by 75-μm C_{18} packed spray tip nanocolumn packed with Michrom Magic C18AQ, for a 2-step gradient. Mobile phase A was water-acetonitrile-formic acid (98%/2%/0.2%), and mobile phase B was acetonitrile-isopropanol-water-formic acid (80%/10%/10%/0.2%). Using a flow rate of 350 nl/min, a 90-min, 2-step LC gradient was run from 5% mobile phase B to 50% mobile phase B in 60 min, followed by 50% to 95% mobile phase B over the next 10 min, a hold for 10 min at 95% mobile phase B, and back to starting conditions, followed by reequilibration.

LC-MS/MS analysis. Samples were analyzed via electrospray tandem mass spectrometry (LC-MS/MS) on a Thermo Q-Exactive Orbitrap mass spectrometer, using a 70,000 RP survey scan in profile mode, *m/z* 350 to 2,000 Da, with lock masses, followed by 20 MS/MS higher-energy collisional dissociation (HCD) fragmentation scans at 17,500 resolution on doubly and triply charged precursors. Single charged ions were excluded, and ions selected for MS/MS were placed on an exclusion list for 60 s. An inclusion list of expected 2+ and 3+ *m/z* tryptic ions was used for a subset of targeted proteins (in-house software). These candidate ions were selected for MS/MS if detected in the MS scan, regardless of their abundance.

Database searching. Tandem mass spectra were extracted by Proteo Wizard version 3.0.6447. All MS/MS samples were analyzed using Mascot (Matrix Science, London, United Kingdom; version 2.3.02) and X! Tandem (The GPM [http://thegpm.org]; version CYCLONE [2010.12.01.1]). Mascot was set up to search the 140401_SPROT_Tetrahymena_thermophila database (unknown version; 24,698 entries) assuming the digestion enzyme trypsin. X! Tandem was set up to search the 140401_SPROT_Tetrahymena_thermophila database. Mascot and X! Tandem were searched with a fragment ion mass tolerance of 0.60 Da and a parent ion tolerance of 20 ppm. Carbamidomethyl of cysteine was specified in Mascot and X! Tandem as a fixed modification. Glu→pyro-Glu of the N terminus, ammonia loss of the N terminus, Gln→pyro-Glu of the N terminus, oxidation of methionine, formyl of the N terminus, and carbamidomethyl of cysteine were specified in X! Tandem as variable modifications. Oxidation of methionine and formyl of the N terminus were specified in Mascot as variable modifications.

Criteria for protein identification. Scaffold (version Scaffold_4.2.1; Proteome Software Inc., Portland, OR) was used to validate MS/MS-based peptide and protein identifications. Peptide identifications were accepted if they could be established at greater than 91.0% probability to achieve a false-discovery rate (FDR) of less than 1.0%. Peptide probabilities from X! Tandem were assigned by the Peptide Prophet algorithm (36) with Scaffold delta-mass correction. Peptide probabilities from Mascot (Ion Score Only) were assigned by the Scaffold Local FDR algorithm. Protein identifications were accepted if they could be established at greater than 99.0% probability to achieve an FDR less than 1.0% and contained at least 2 identified peptides. Protein probabilities were assigned by the Protein Prophet algorithm (37). Proteins that contained similar peptides and could not be differentiated based on MS/MS analysis alone were grouped to satisfy the principles of parsimony.

RESULTS

Cth4p, a cysteine cathepsin, is a strong candidate for a mucocyst processing enzyme based on expression profiling. In prior work, we mined an expression database of *T. thermophila* transcripts to

discover that a set of genes encoding mucocyst cargo proteins, a *VPS10* family receptor involved in cargo sorting, and several putative proteases were all transcriptionally coregulated (16, 27, 34). Among those proteases is a gene for cathepsin 4 (*CTH4*), whose expression pattern was strikingly similar to that of several other mucocyst-associated genes (Fig. 1A). A phylogram including *CTH4* and related genes in other organisms, which were identified as top BLAST hits, shows that *CTH4* falls within the genes for the family of cysteine cathepsins, including cathepsin C in *H. sapiens* (labeled Hs 8-9) (Fig. 1B). *CTH4* is only distantly related to *CTH3*, the gene for an aspartyl cathepsin previously shown to be involved in mucocyst proprotein processing (see Fig. S1 in the supplemental material). In addition, the genes most closely related to *CTH4* in the *T. thermophila* genome show a different expression pattern, suggesting that *CTH4* is unlikely to have a functionally redundant paralog (Fig. 1A).

Cth4p-CFP, expressed from an inducible promoter, localizes to cytoplasmic puncta and docked mucocysts. We expressed a copy of Cth4p, with cyan fluorescent protein (CFP) appended to the C terminus, under the transcriptional control of the inducible *MTT1* promoter, in order to visualize both initial and potentially processed products (38). Western blotting of cell lysates after 30, 60, and 120 min of induction, using an anti-GFP antibody, showed a protein of the expected size, as well as a polypeptide of the size expected for monomeric CFP (Fig. 2A). This pattern is similar to cleavage in *Tetrahymena* of a GFP-tagged variant of Cth3p, releasing monomeric GFP (27).

To determine whether Cth4p localizes to mucocyst intermediates and/or mature organelles, we fixed and permeabilized cells at time points shown in Fig. 2A and then dually labeled them with antibodies against GFP and a mucocyst cargo protein, Grl3p (Fig. 2B). Cth4p-CFP colocalized extensively with Grl3p in docked mucocysts after 120 min but less clearly at the earlier time points when Cth4p-CFP was found primarily in cytoplasmic puncta. An ambiguous feature of these results, explored further below, was that CFP signal in mucocysts at 120 min might reflect the localization of monomeric CFP that is proteolytically cleaved from the chimeric protein and which may be different from that of Cth4p-CFP.

Cth4p-GFP, expressed at the endogenous locus, shows partial overlap with endolysosomal markers. The cysteine cathepsin family contains numerous members in other eukaryotes that function in endolysosomal compartments, which may be represented by the Cth4p-positive cytoplasmic puncta noted above (39). To examine this possibility, we first expressed Cth4p-GFP at the endogenous *CTH4* locus, under its native promoter, to avoid potential overexpression artifacts. Western blotting of cell lysates, using an anti-GFP antibody, showed both full-length protein and monomeric GFP (Fig. 3A). By live imaging, such cells showed strong GFP signals in docked mucocysts (Fig. 3B and C). In addition, live cells also bore a number of GFP-positive cytoplasmic puncta, whose number and appearance depended on culture density. We imaged such cells after incubation with either FM4-64, which labels endocytic compartments (40), or Lysotracker Red (Fig. 3D and E). In both cases, the GFP-positive puncta showed clear albeit incomplete overlap with the endolysosomal markers.

Monomeric GFP, but not Cth4p-GFP, accumulates in docked mucocysts. The Western blot results in Fig. 2A indicate that puncta in cells expressing Cth4p-GFP report the localization of both the full-length protein and also monomeric GFP generated by cleavage. These species may not colocalize entirely, if they undergo separate sorting following the cleavage. To determine whether full-length Cth4p-GFP is present in docked mucocysts, we stimulated cells expressing Cth4p-GFP (cth4-2p, from the endogenous locus) to release their docked mucocysts via exocytosis and analyzed the poststimulated, mucocyst-depleted cells by Western blotting using anti-GFP and anti-Grl1p antibodies. There was no detectable release of GFP into the cell culture medium of nonstimulated cells (data not shown). For the stimulated samples, we found that monomeric GFP, but not full-length Cth4p-GFP, was depleted from cells by dibucaine stimulation, indicating that only the former is present in mature mucocysts (Fig. 4). These results explain the difference between the intensity of mucocyst labeling in cells continuously expressing Cth4p-GFP (Fig. 3) versus those in which short-term expression was induced (Fig. 2), since in the former there is a large pool of accumulated monomeric GFP cleaved from the full-length protein.

Taken together, our results show that Cth4p localizes partially to endolysosomal compartments, while GFP that has been cleaved from Cth4p-GFP accumulates in mature mucocysts. Importantly, GFP with an N-terminal signal sequence shows no localization to mucocysts (22). Therefore, the targeting of GFP to mucocysts in strains expressing Cth4p-GFP must depend on signals present in Cth4p, prior to cleavage of the chimeric protein. These results can be explained if some cleavage of GFP from Cth4p occurs in immature mucocysts and free GFP is retained during subsequent mucocyst maturation while Cth4p-GFP and Cth4p are retrieved. In addition, our results do not rule out the possibility that some cleavage of GFP from Cth4p-GFP occurs in docked mucocysts, in which Cth4p may also be retained.

***CTH4* knockout results in a marked defect in mucocyst exocytosis.** To determine whether *CTH4* is required for mucocyst function, we replaced the open reading frame of the gene with a drug resistance cassette via homologous recombination (Fig. 5A). We obtained cells with no detectible *CTH4* transcript, indicating that all copies of the gene in the somatic macronucleus had been disrupted (Fig. 5B). Therefore, the gene is not essential, and such Δ*cth4* cells had a doubling time indistinguishable from that of the wild type (data not shown).

We exposed Δ*cth4* cells to dibucaine, a secretagogue that induces rapid synchronous mucocyst exocytosis (Fig. 5C) (41). In wild-type cells, the core proteins in mucocysts assemble as a crystal roughly 1 μm in length, which upon exocytosis undergoes dramatic expansion to ~7 μm (20). As a result, stimulation followed by low-speed centrifugation results in a visible layer of sedimenting flocculent, made up of the expanded and released mucocyst cores (Fig. 5D). In contrast, we found that stimulation of Δ*cth4* cells resulted in a much smaller flocculent layer, indicating that the gene is required for efficient mucocyst synthesis or exocytosis. Together with the aspartyl cathepsin encoded by *CTH3*, the enzyme encoded by *CTH4* is thus a second enzyme implicated in mucocyst function.

***CTH4* is not required for formation and accumulation of docked mucocysts but is required for efficient core extrusion upon exocytosis.** *T. thermophila* that lacks *CTH3* accumulates a reduced number of mucocysts, which are also morphologically aberrant (27). These defects explained why Δ*cth3* cells show negligible release of mucocyst contents upon exocytic stimulation. Surprisingly, Δ*cth4* cells showed no apparent defect in mucocyst formation, notwithstanding the clear exocytosis phenotype. We immunostained the cells with antibodies against two different

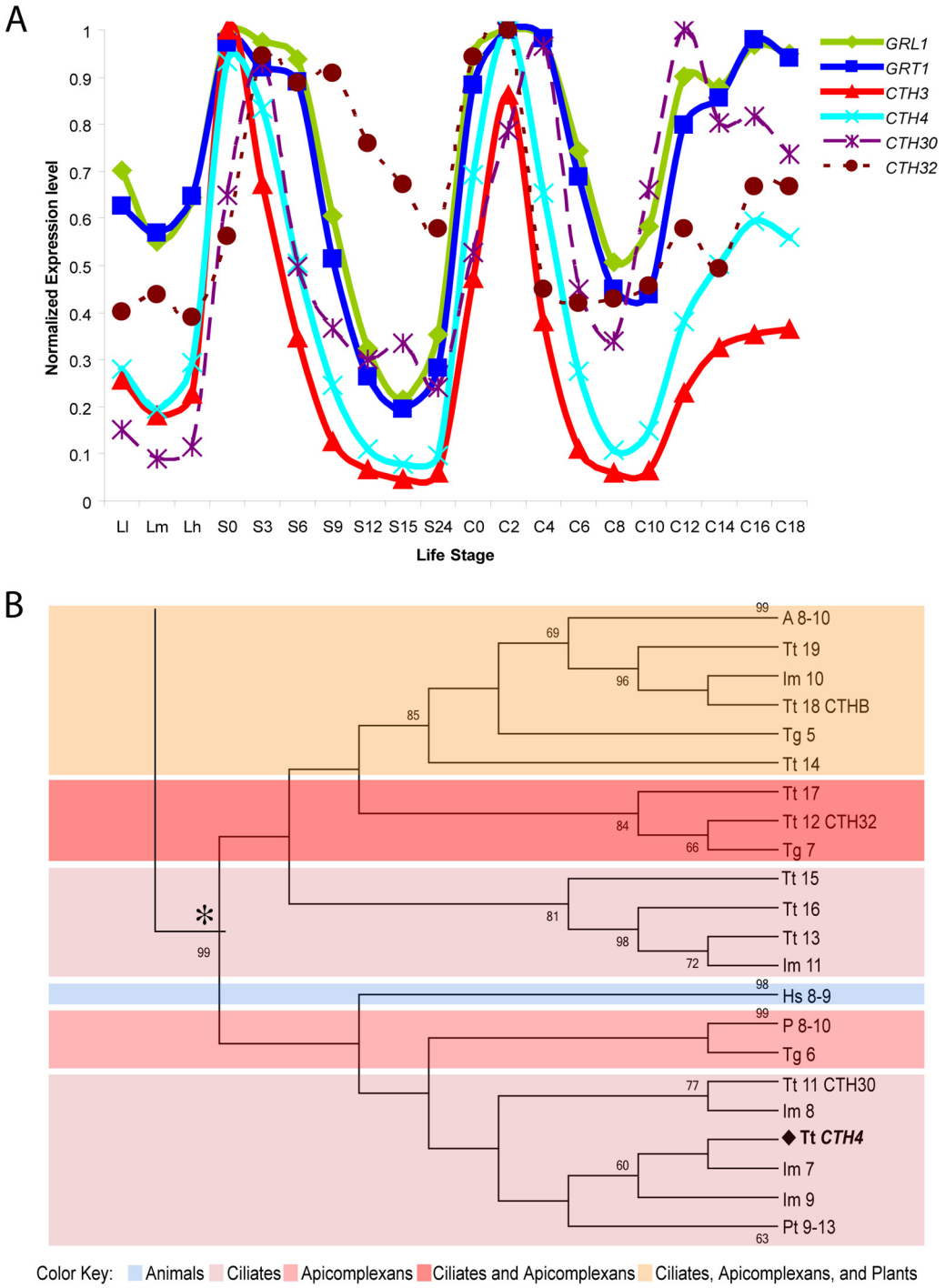

FIG 1 (A) The expression profile of *CTH4* is very similar to those of genes required for mucocyst biogenesis: *GRL1*, *GRT1*, and *CTH3*. In contrast, the expression profiles of two genes that are sequence related to *CTH4*, *CTH30* (TTHERM_00502690) and *CTH32* (*TTHERM_01248970*), show less overlap with those of mucocyst-associated genes. The profiles of transcript abundance under a variety of culture conditions, derived via hybridization of cDNAs to whole-genome microarrays, were downloaded from the *Tetrahymena* Functional Genomics Database (http://tfgd.ihb.ac.cn/). In the plots shown here, each trace was normalized to that gene's maximum expression level. The culture conditions sampled at successive time points represent growing (Ll, Lm, and Lh), starved (S0, S3, S6, S9, S12, S15, and S24), and conjugating (C0, C2, C4, C6, C8, C10, C12, C14, C16, and C18) cultures (28). (B) Phylogenetic reconstruction of cysteine cathepsin genes. The maximum likelihood tree illustrates the phylogenetic relationship between cysteine cathepsins in ciliates, apicomplexans, *Arabidopsis* species, and *Homo sapiens*. The *T. thermophila* cysteine cathepsin *CTH4* is emboldened. For key to color blocks, see the bottom. Abbreviations: Tg, *Toxoplasma gondii*; P, *Plasmodium*; A, *Arabidopsis*; Hs, *Homo sapiens*; Tt, *Tetrahymena thermophila*; Pt, *Paramecium tetraurelia*; Im, *Ichthyophthirius multifiliis*. The tree shown was assembled with aspartyl cathepsins as the outgroup; see Fig. SA1 in the supplemental material for complete tree. See Table SA2 for accession numbers.

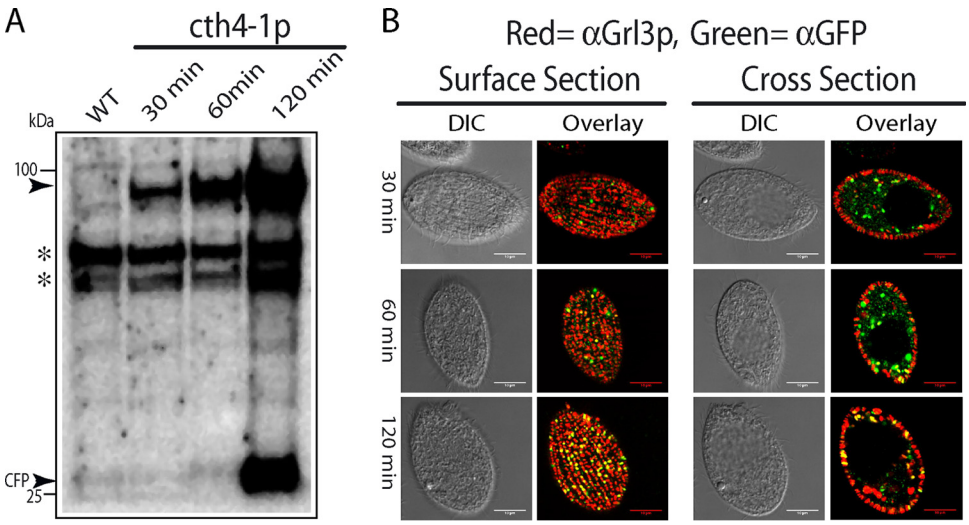

FIG 2 Expression and localization of CFP-tagged Cth4p. (A) Western blot, probed with anti-GFP MAb that cross-reacts with CFP, of cells expressing CFP-tagged Cth4p (cth4-1p). cth4-1p expression was induced for 30, 60, and 120 min with 1 μg/ml of $CdCl_2$. At these times, cell lysates were prepared by trichloroacetic acid (TCA) precipitation and then solubilized in SDS-PAGE sample buffer. Proteins fractions were separated by 4 to 20% SDS-PAGE and transferred to polyvinylidene difluoride (PVDF). Molecular mass standards are shown on the left. The specific bands recognized by the antibody, indicated by arrowheads, are of the size expected for full-length Cth4p-CFP (94 kDa) and monomeric CFP. At 30 and 60 min of induction, only full-length Cth4p-CFP was detected, whereas monomeric CFP was also detected after 120 min. Asterisks indicate nonspecific cross-reactive species. (B) Using the same cultures as for panel A, cells at 30, 60, and 120 min were fixed and immunolabeled with mouse MAb 5E9 to localize mucocyst protein Grl3p and rabbit anti-GFP to localize the Cth4p-CFP fusion. The fluorescent puncta at the cell surface, which appear as elongated vesicles in cross section, correspond to the array of docked mucocysts. Scale bars = 10 μm.

mucocyst markers, and both revealed docked mucocysts indistinguishable from those of the wild type at the level of light microscopy (Fig. 6A). Similarly, electron microscopy of thin sections revealed uniformly elongated mucocysts, demonstrating that Cth4p activity is not required for the assembly of the crystalline mucocyst core (Fig. 6B).

Since Δ*cth4* cells accumulate mucocysts, their secretion defect suggested that Δ*cth4* mucocysts are incapable of undergoing efficient exocytosis. To investigate this possibility, we visualized both wild-type and mutant cells that were fixed immediately following stimulation with the secretagogue alcian blue (42), using antimucocyst antibodies and immunofluorescence or electron microscopy (Fig. 7A, B, and D). Because this secretatogogue also binds tightly to secreted mucocyst proteins, a subset of the alcian blue-treated wild-type *Tetrahymena* becomes trapped in capsules formed by cross-linked, extruded mucocyst cores, which are highly immunoreactive (Fig. 7B, 3rd row). A second pool of stimulated wild-type cells showed virtually no antibody reactivity in the cells, consistent with previous observations that synchronous exocytosis of all docked mucocysts is complete within seconds (43) (Fig. 7B, 4th row). These two pools could be clearly resolved by flow cytometry (Fig. 7C). The Δ*cth4* samples appeared identical to the wild type prior to stimulation (Fig. 7B, top rows) but still showed very substantial immunostaining within the cells after stimulation, indicating that many mucocyst cores had not been fully released (Fig. 7B, bottom row). This was confirmed by flow cytometry (Fig. 7C). In addition, Δ*cth4* cells failed to form any alcian blue-staining capsules (Fig. 7B, bottom row, and Fig. 7C). The Δ*cth4* mucocysts that were retained in stimulated cells no longer appeared elongated by light microscopy (Fig. 7B, bottom row, inset). Electron microscopy of Δ*cth4* cells after stimulation confirmed that cores had become roughly spherical (Fig. 7D). Thus, while Δ*cth4* mucocysts respond to cell stimulation by secretagogues, both the core expansion and its functional consequences are distinct from those in wild-type mucocysts.

The partial release of contents from Δ*cth4* cells could be accounted for by complete failure of some mucocysts to undergo exocytosis, or partial failure of all mucocysts. Both light and electron microscopy data suggested the latter, implying that individual Δ*cth4* mucocysts only released a portion of their cargo upon stimulation. One striking feature of a wild-type mucocyt core is that as it undergoes ~7-fold expansion upon extrusion from stimulated cells, the Grl proteins remain organized in an extended, very stable lattice (20). Thus, partial release of a mucocyst core could occur only if the lattice itself were unstable and could fragment during exocytosis.

To investigate this possibility, we exploited the fact that even following release, wild-type Grl proteins persist in large stable complexes (44). Indeed, this property is the basis of the formation of the sedimenting flocculent layer described above. To determine if this property is conserved in Δ*cth4* mucocyst cores, we stimulated Δ*cth4* cells to undergo exocytosis and then centrifuged the sample using conditions that sediment Grl proteins in wild-type samples. We then used Western blotting to analyze the distribution of Grl proteins in the flocculent layer versus the supernatant. In the Δ*cth4* samples, much of the protein was found in the nonpelleting fractions (Fig. 8). The difference between wild-type and Δ*cth4* samples therefore suggests that some interactions between Grl proteins depend on the activity of Cth4p during core assembly. In addition, the Western blots suggested that processing of mature Grl proteins was incomplete in Δ*cth4* cells, as indicated by slight shifts in electrophoretic mobility and as detailed below.

***CTH4* is required for full processing of proGrl proteins.** Formation of mucocyst cores is controlled by proteolytic maturation

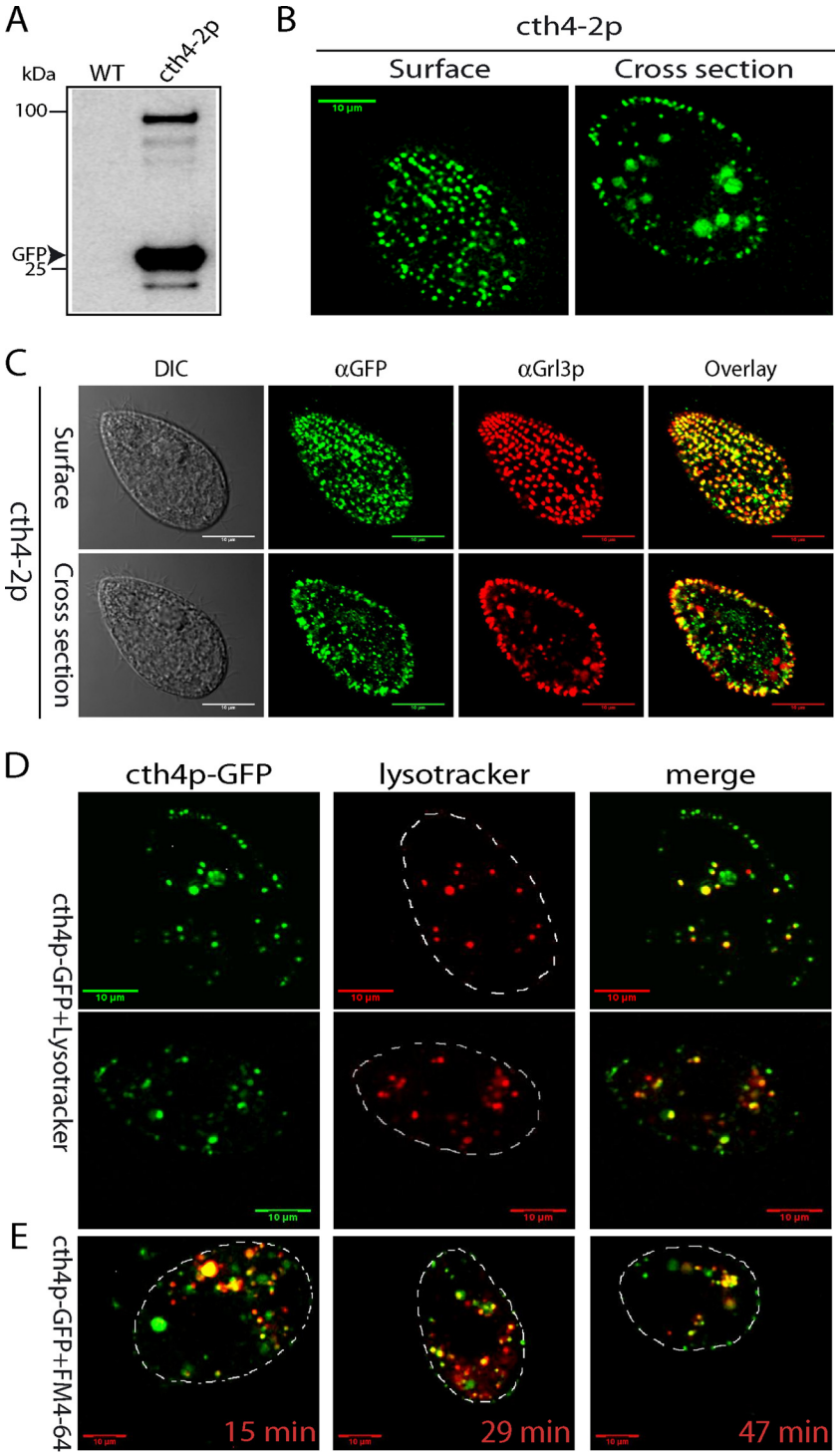

FIG 3 Localization of endogenous Cth4p-GFP. (A) Expression of *cth4-2*: GFP-tagged Cth4p from the endogenous *CTH4* locus, under the control of its native promoter. cth4-2p was immunoprecipitated from detergent lysates using polyclonal rabbit anti-GFP antiserum, and immunoprecipitates were Western blotted with monoclonal anti-GFP Ab. One immunoreactive band is of the size expected for the Cth4p-GFP fusion, while a second is the size expected for monomeric GFP. (B) Live immobilized cells expressing cth4-2p were imaged to capture cell surface and cross sections and show the expected array of docked mucocysts as well as intracellular puncta. (C) Immunostaining of fixed cells to simultaneously localize mucocyst protein Grl3p and cth4-2p. There is extensive colocalization in docked mucocysts, while some puncta deeper in the cytoplasm are positive for cth4-2p but not Grl3p. (D) Cells were incubated for 5 min with 200 nM Lysotracker, and live images were captured within 30 min. Optical sections shown are cell cross sections. (E) Cells were incubated for 5 min with 5 μM FM4-64, an endocytic tracer and then pelleted and resuspended in tracer-free medium. The times shown represent minutes after resuspension. Scale bars = 10 μm.

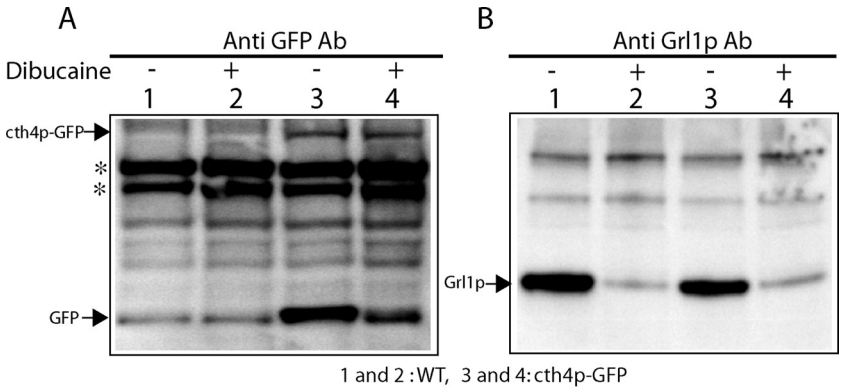

FIG 4 Monomeric GFP, but not Cth4p-GFP, is released upon mucocyst exocytosis. Fifty-milliliter cultures of wild-type or cth4p-GFP expressing cells (from the endogenous locus) were first grown overnight to ~3 × 10^5/ml at 30°C in SPP and then incubated for an additional 24 h at 22°C with gentle shaking. Two 15-ml samples were removed from each culture and pelleted and resuspended in 1.5 ml of medium, and one half were treated with dibucaine for 20 s. The cells were then diluted to 15 ml and centrifuged to generate cell pellet, flocculent, and supernatant fractions as in Fig. 5. After aspiration of the superatants, tubes were sliced with a razor below the flocculent-cell interface, and the flocculent was discarded. Cells were resuspended in 10 mM Tris (pH 7.4), repelleted, and then lysed with 10%TCA. Lysates (5 × 10^4 cell equivalents) were resolved by 4 to 20% SDS-PAGE, transferred to PVDF, and Western blotted with anti-GFP (A) or anti-Grl1p (B) antibody. (Left blot) No release of cth4p-GFP from cells is seen, since the band intensities are equivalent in untreated and dibucaine-treated cells. In contast, a substantial fraction of free GFP is released by dibucaine stimulation. (Right blot) Grl1p is released from wild-type or cth4p-GFP cells during dibucaine stimulation.

of the Grl proteins (45). Since Cth4p is predicted to act as a protease, the defects in Δ*cth4* mucocysts may be due to defects in pro-Grl processing. Consistent with this idea, Western blots of Δ*cth4* whole-cell lysates with antibodies against Grl1p revealed clear differences from the wild type. First, the Δ*cth4* cells accumulated higher levels of the unprocessed precursor than did the wild type (Fig. 9A). Second, Δ*cth4* cells also accumulated a processed Grl1p product, but this species had slightly lower mobility on

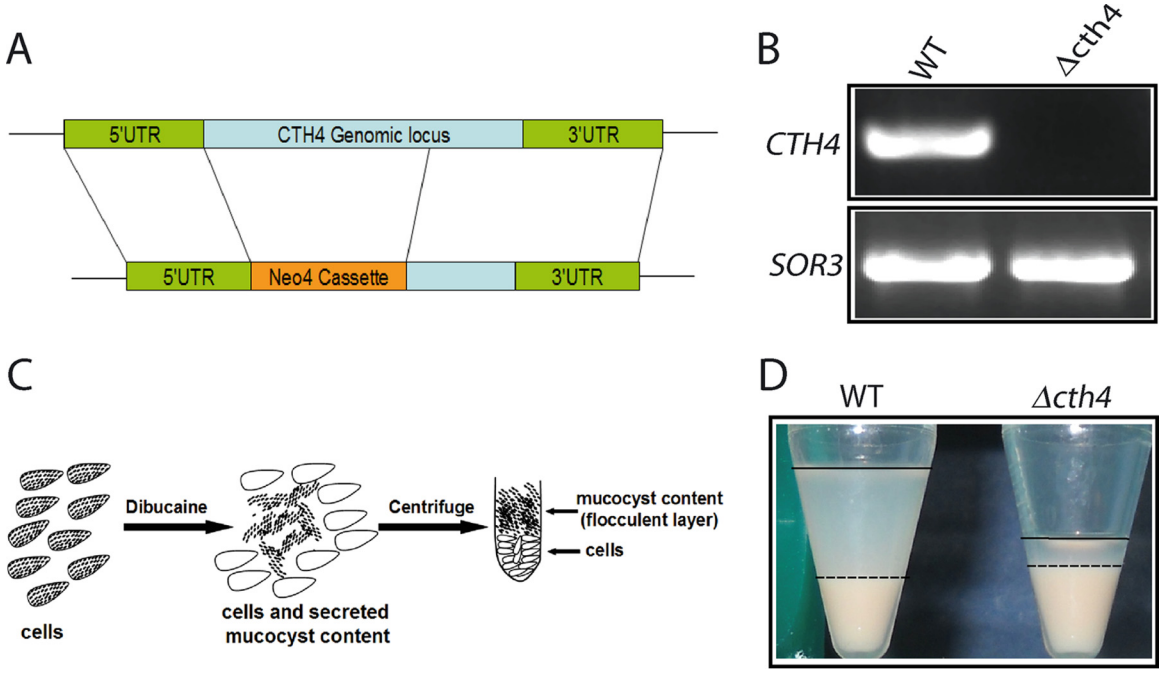

FIG 5 *CTH4* is required for normal mucocyst discharge. (A) Schematic of *CTH4* gene knockout construct. Replacement of the *CTH4* gene by the Neo4 drug resistance cassette, to generate Δ*cth4*, was targeted by homologous recombination. (B) Verification of gene knockout by RT-PCR. RNA was extracted from wild-type (WT) and Δ*cth4* cells, subjected to coupled reverse transcription, and PCR amplified using primers listed in Table S1 in the supplemental material. As shown in this 1% ethidium bromide-stained agarose gel, Δ*cth4* cells lacked any detectible products corresponding to the targeted gene. *SOR3* provides a positive control. (C) Illustration of semiquantitative assay for mucocyst discharge. Cells were stimulated with dibucaine for 20 s, which triggers synchronous exocytosis of mucocyst contents. Subsequent centrifugation results in a dense pellet of cells, with an overlying flocculent comprised of expanded cores of exocytosed mucocysts. (D) Stimulated WT cell cultures generate the expected two-layered pellet (left). For clarity, the flocculent layers are delineated with a dashed line at the lower border and an unbroken line at the upper border. Stimulated Δ*cth4* cultures produce a greatly reduced amount of flocculent (right). Although identical numbers of cells were used in all samples, the poststimulation wild-type cell pellet is smaller because some cells have remained trapped in the sticky flocculent layer.

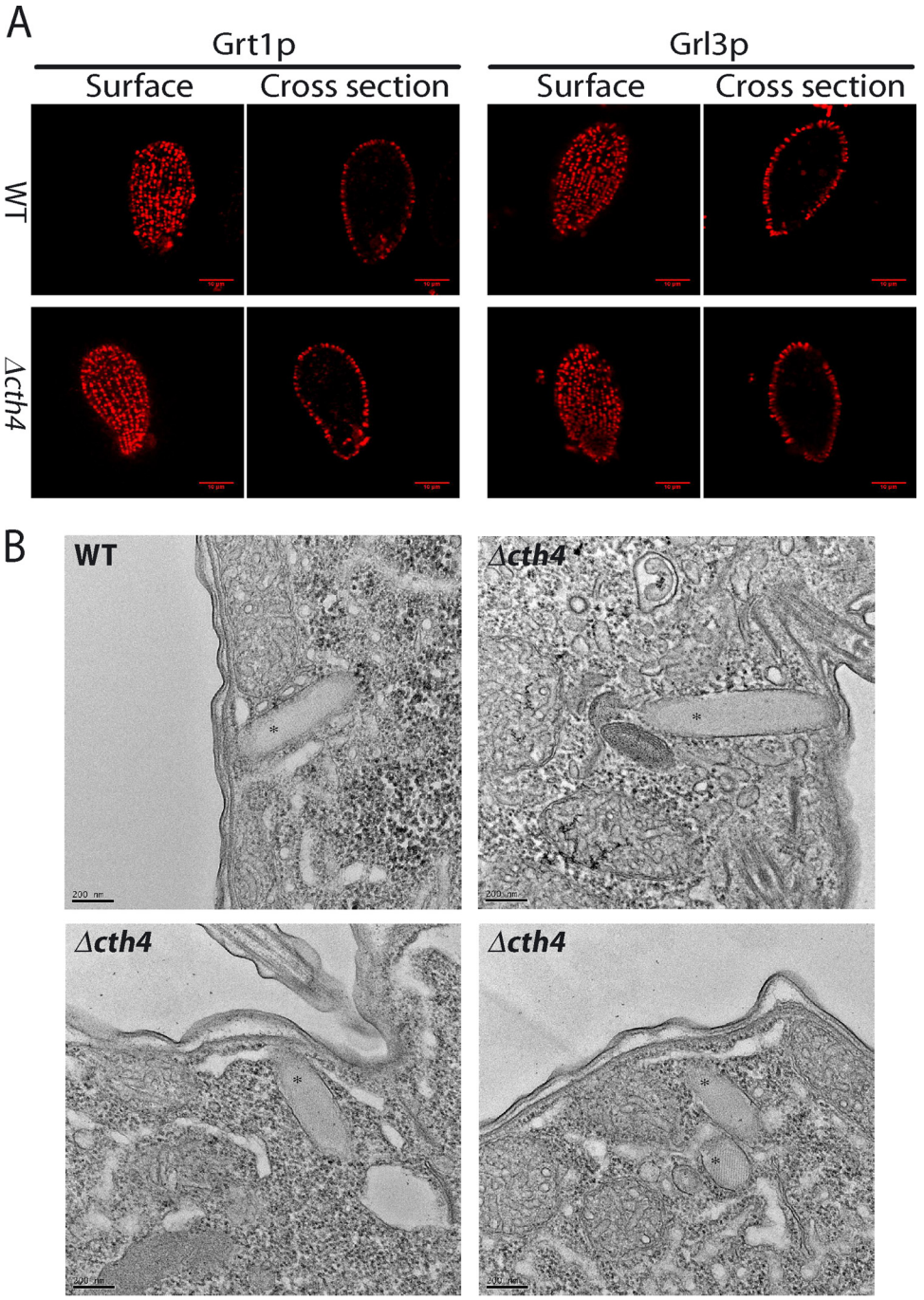

FIG 6 *CTH4* is not required for formation and accumulation of docked mucocysts. (A) (Top) docked mucocysts in fixed wild-type cells, immunolabeled using MAb 4D11, which recognizes Grt1p (left two images), and MAb 5E9, which recognizes Grl3p (right two images). Shown are optical surface and cross sections. (Bottom) parallel immunostaining of Δ*cth4* cells shows patterns indistinguishable from the wild type. Scale bars = 10 μm. (B) Electron micrographs of mucocysts (labeled with asterisks) in wild-type and Δ*cth4* cells. The mucocyst cores in both wild-type and Δ*cth4* cells are organized as visible lattices. Scale bars = 0.2 μM.

SDS-PAGE than the corresponding band in wild-type lysates (Fig. 9A). The same pattern was also seen for a second Grl protein, Grl3p (Fig. 9B).

The accumulation of unprocessed proGrl precursors has been noted in a variety of mutants affecting mucocyst function (46; unpublished data), but accumulation of a larger-than-wild-type final product has not previously been observed, and it suggested the existence of a previously overlooked processing step. To investigate this possibility, we isolated the secreted contents of both wild-type and Δ*cth4* cells, i.e., the flocculent layer following stimulation. The material was separated by SDS-PAGE, from which we excised gel regions that were expected to contain processed Grl

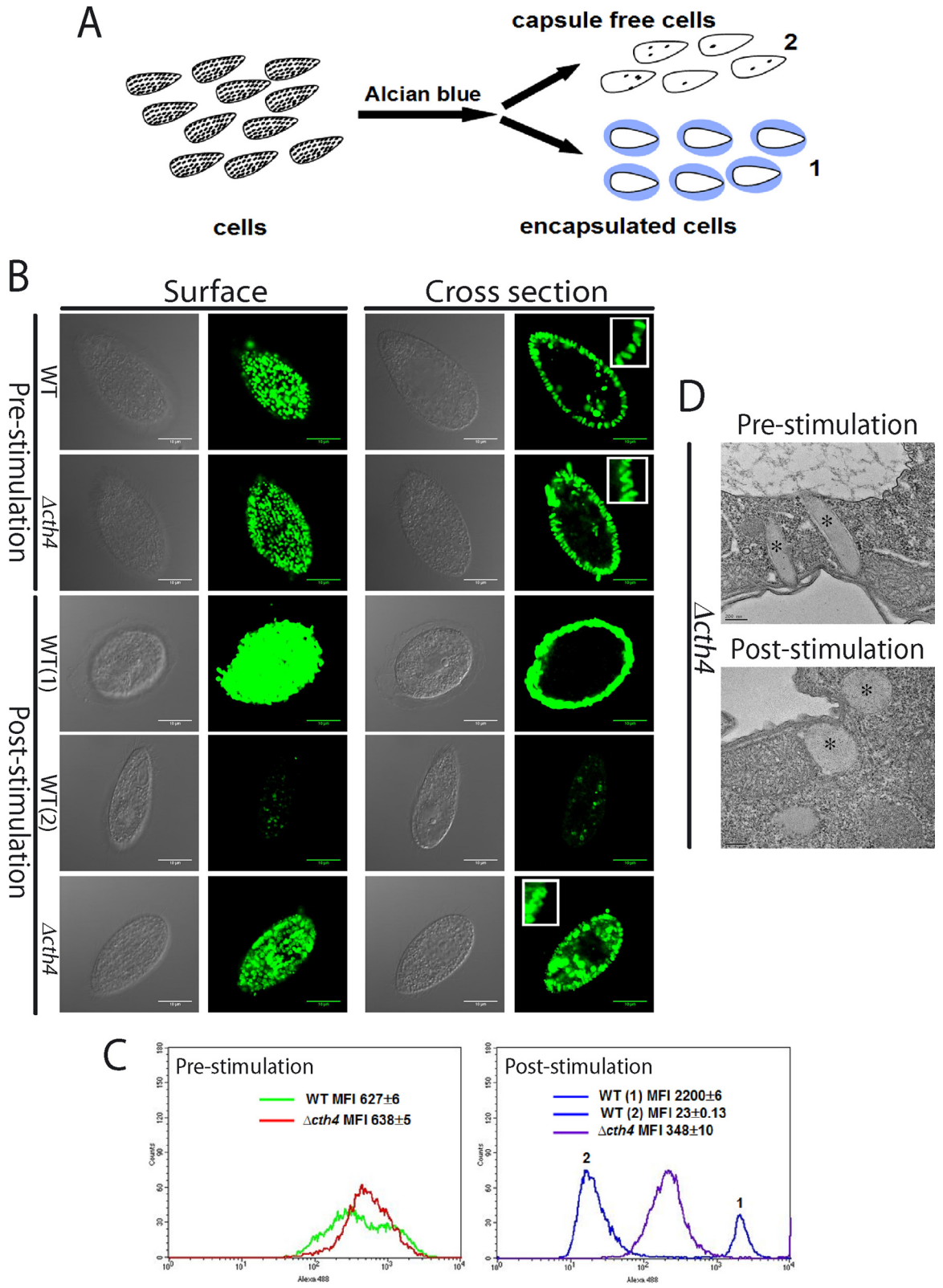

FIG 7 *CTH4* is required for efficient cargo release upon exocytosis. (A) Illustration of qualitative assay for mucocyst discharge. Cells are stimulated by addition of alcian blue, which triggers mucocyst exocytosis and binds to released mucocyst proteins, resulting in two distinct pools of cells. Cells in pool 1 are individually trapped by translucent capsules formed by released mucocyst contents, while cells in pool 2 are not entrapped because they have already escaped from their capsules. (B and C) Cells, before and after stimulation with alcian blue, were fixed, detergent permeabilized, immunolabeled with MAb against Grl3p, and then analyzed by confocal microscopy or flow cytometry. (B) Wild-type and Δ*cth4* cells prior to stimulation display identical docked mucocysts, visible as discrete puncta (top two rows). After stimulation, wild-type cells are surrounded by translucent capsules of released mucocyst contents, distinct from the punctate

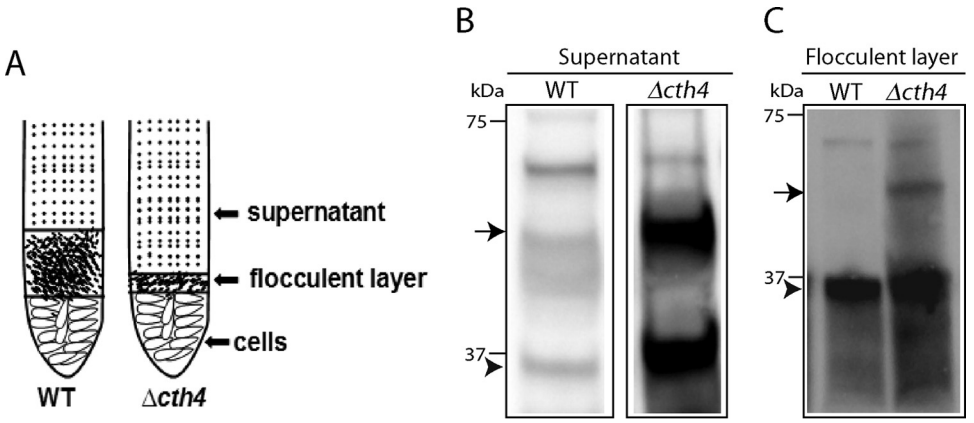

FIG 8 Secreted mucocyst contents from Δ*cth4* cells show increased solubility. (A) Illustration of samples following dibucaine stimulation of WT and Δ*cth4* cultures. Two-milliliter quantities of supernatants were withdrawn and precipitated with TCA, while 20-μl quantities of the flocculent layers were directly dissolved in SDS-PAGE buffer. (B and C) Western blots, using antibodies against Grl1p. The arrow indicates proGrl1p, and the arrowhead indicates processed Grl1p. (B) Supernatant fractions; (C) flocculent fractions. Δ*cth4* cells release both proGrl1p and mature Grl1p, with much of the protein found in the nonpelleting supernatant fraction. The comparison between flocculent sample lanes in WT versus Δ*cth4* cultures does not indicate similar amounts of release, since the volume of flocculent released by WT cultures is much greater than by Δ*cth4* cultures.

proteins (Fig. 9C). This material was analyzed by mass spectrometry. We focused on peptides derived from pro-Grl proteins, which are encoded by a small gene family (22). Importantly, we had previously used Edman degradation to establish the N termini of five of the mature Grl products, derived from proGrl1p, -3p, -4p, -5p, and -7p (20).

Concentrating on these five Grl proteins, we found additional peptides in the Δ*cth4* samples compared to the wild type. These peptides, mapped to the full-length protein sequence, corresponded to extensions from the mature Grl N termini characterized in wild-type cells (Fig. 9D). We found such extensions for five of the six previously mapped N termini. Thus, the absence of Cth4p leads to N-terminally elongated Grl products, which is consistent with the shift to larger sizes seen by SDS-PAGE and Western blotting. Since *CTH4*-related cathepsins in other organisms can act as aminopeptidases, one possibility is that Cth4p is required for N-terminal trimming of Grl processing intermediates. Our data do not establish the precise extensions present in Δ*cth4* cells, since the amino termini of the peptides detected are produced by trypsin treatment during preparation of the mass spectrometry samples.

***In vivo CTH4* function depends on conserved enzymatic residues.** The polypeptide corresponding to *CTH4* includes the residues, conserved among related papain-family enzymes, which are directly involved in substrate hydrolysis (39) (Fig. SA2). If Cth4p acts *in vivo* as an enzyme, mutating the conserved enzymatic residues should be functionally equivalent to gene disruption. We therefore used site-specific mutagenesis to substitute the conserved active site cysteine and histidine and replaced the endogenous gene with the mutated allele via homologous recombination followed by drug selection (Fig. 10A). In addition, we added a C-terminal GFP tag to detect the novel product. We compared this construct to a similarly GFP-tagged allele of the wild-type gene, also expressed via gene replacement at the endogenous locus.

Both the wild-type and enzymatically disabled alleles were expressed as products of the expected sizes, judging by SDS-PAGE (Fig. 10B). Western blotting of whole-cell lysates demonstrated that cells expressing the site-specifically mutated allele showed the same upward shift in the size of processed Grl products as seen in Δ*cth4* cells (Fig. 10C and D). In addition, cells expressing mutated Cth4p showed a clearly defective secretory response upon secretagogue stimulation, indistinguishable from the response of Δ*cth4* cells (Fig. 10E). The processing and secretion defects were not due to mistargeting of the disabled protein, since localization was not distinguishable from that of the wild-type, GFP-tagged protein (Fig. 10F). These results are therefore consistent with the ideas that Cth4p acts enzymatically and that the defects in Δ*cth4* cells are due to the absence of Cth4p catalytic activity during mucocyst formation.

Cth4p undergoes *CTH3*-dependent processing. A model based on studies with Cth3p and Cth4p, the two enzymes now implicated in proGrl processing, is shown in Fig. 11. Based primarily on the gene knockout phenotypes, *CTH3* appears to act upstream of *CTH4*, and we propose that Cth4p directly trims the products generated by Cth3p. Because the proGrl sites recognized and cleaved by Cth3p are as yet unknown, we are not yet in a position to test such products *in vitro* as potential Cth4p substrates. The precise sites of Cth3p cleavage cannot be inferred from

mucocyst staining prior to stimulation, that stain brightly for Grl3p (pool 1, 3rd row) or are largely devoid of Grl3p staining (pool 2, 4th row). Stimulated Δ*cth4* cells do not form capsules and still display abundant docked mucocysts (bottom row), though different in appearance from prestimulation samples. Scale bars = 10 μm. Insets in right-hand panels: rows 1 and 2, elongated docked mucocysts in WT and Δ*cth4* cells prior to stimulation; row 5, irregular mucocyst profiles in Δ*cth4* cells following stimulation. (C) Flow cytometry of wild-type and Δ*cth4* cells, before and after stimulation. (Left graph) prior to stimulation, WT and Δ*cth4* cells show similar labeling with anti-Grl3p Ab. (Right graph) after stimulation, WT cells show two distinct populations, corresponding to pools 1 and 2. Poststimulation Δ*cth4* cells instead show a single population, whose staining intensity suggests that roughly half of Grl3p was released by exocytosis. For flow cytometry, 10^4 cells/sample were analyzed. MFI, mean fluorescence intensity. (D) Electron micrographs of docked mucocysts (*) in Δ*cth4* cells, fixed before and after alcian blue stimulation. Scale bars = 0.2 μm.

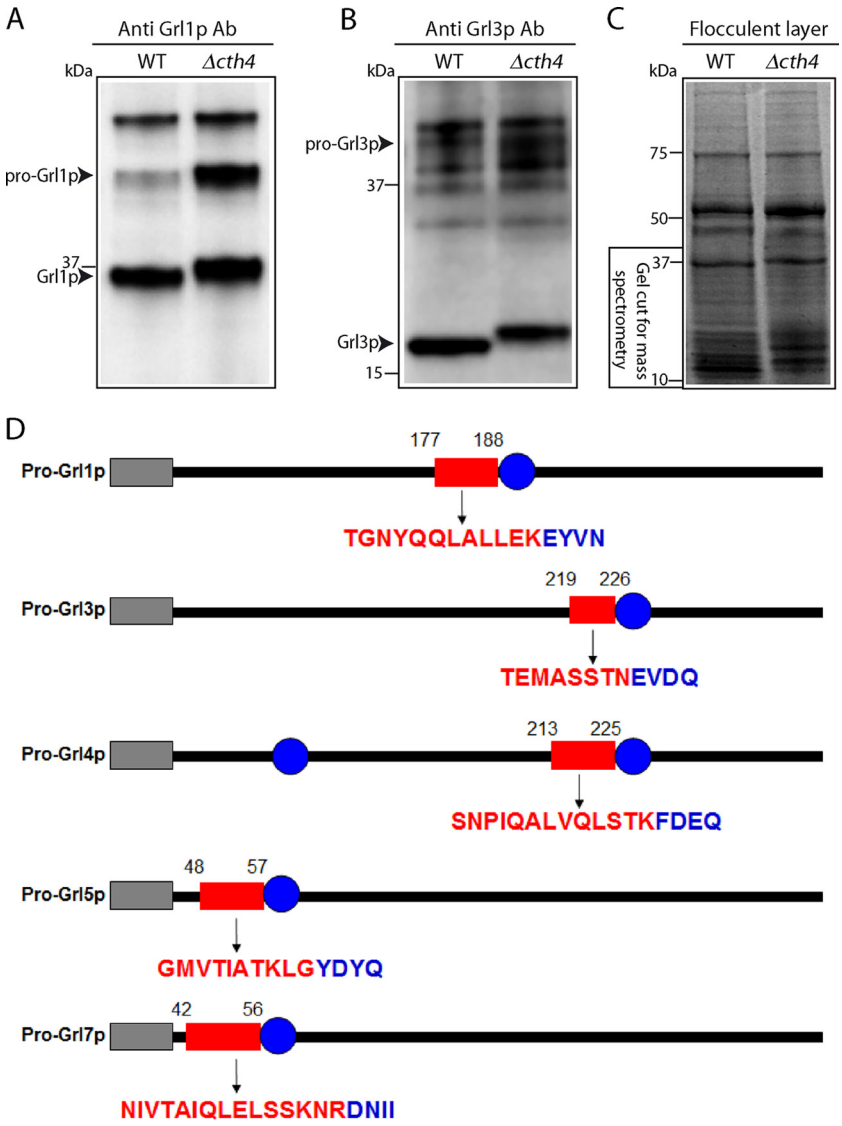

FIG 9 *CTH4* is required for full processing of Grl proteins. Cell lysates (5×10^3 cell equivalents in panel A and 10^4 cell equivalents in panel B) were resolved by SDS-PAGE (10% [A] and 4 to 20% [B]), transferred to PVDF, and Western blotted with antibodies against Grl proteins. The unprocessed (proGrl) and processed (Grl) bands are labeled. (A) Blotting with anti-Grl1p antibody. The predominant band in WT lysates (lane 1) is mature processed Grl1p. The corresponding band in Δ*cth4* lysates is shifted slightly in mobility, and the lysate also shows a high level of unprocessed precursor. (B) Same as panel A, but blotting with anti-Grl3p antibody. (C) Gel (4 to 20%) stained with Coomassie brilliant blue, containing flocculent samples from dibucaine-stimulated WT and Δ*cth4* cultures. Molecular mass standards are shown on the left. The gel regions excised for mass spectrometry are shown. (D) The processed Grl products retain N-terminal extensions in Δ*cth4* cells. Each of the proGrl genes shown begins with an N-terminal signal sequence (gray rectangle) and has either one (for Grl1, -3, -5, and -7) or two (for Grl4) sites (blue circles) that were previously established as N termini of processed Grl products isolated from extruded wild-type mucocysts (20). The red rectangles represent the positions of peptides present in Δ*cth4* samples but not the wild-type samples. In each case, the peptide constitutes an amino-terminal extension to the N terminus in proteins isolated from wild-type cells. The amino acids within the Δ*cth4*-specific peptides are shown below the corresponding rectangles in red, while the adjacent amino acids in blue are those at the beginning of the mature polypeptide in wild-type cells.

the mass spectrometry results shown above, since the N termini of the newly identified Δ*cth4*-dependent peptides were generated by trypsin used in processing the gel samples, rather than by proGrl maturases *in vivo*.

In many organisms, cathepsins and other proteolytic enzymes are synthesized as zymogens and attain full activity toward their substrates only after they are themselves processed (47). Cth4p cannot be essential for activation of Cth3p, since *CTH3* disruption resulted in more profound processing defects than *CTH4* disruption (27). Another possibility is that Cth3p is involved in activation of Cth4p, consistent with their proposed order of action in Fig. 11. Cathepsin C family members, including the *Toxoplasma gondii* enzyme most closely related to Cth4p, are comprised of 5 recognized domains: a signal peptide, an exclusion domain, a internal proregion, and finally a catalytic heavy and light chain (Fig. 12A) (48). In the comparatively well-studied mammalian cathepsin C, it is known that the first three domains are removed in a maturation process, to generate a catalytically active heavy+light chain (HL) species (49). In order to detect potential processing intermediates of *T. thermophila* Cth4p, we expressed a copy that

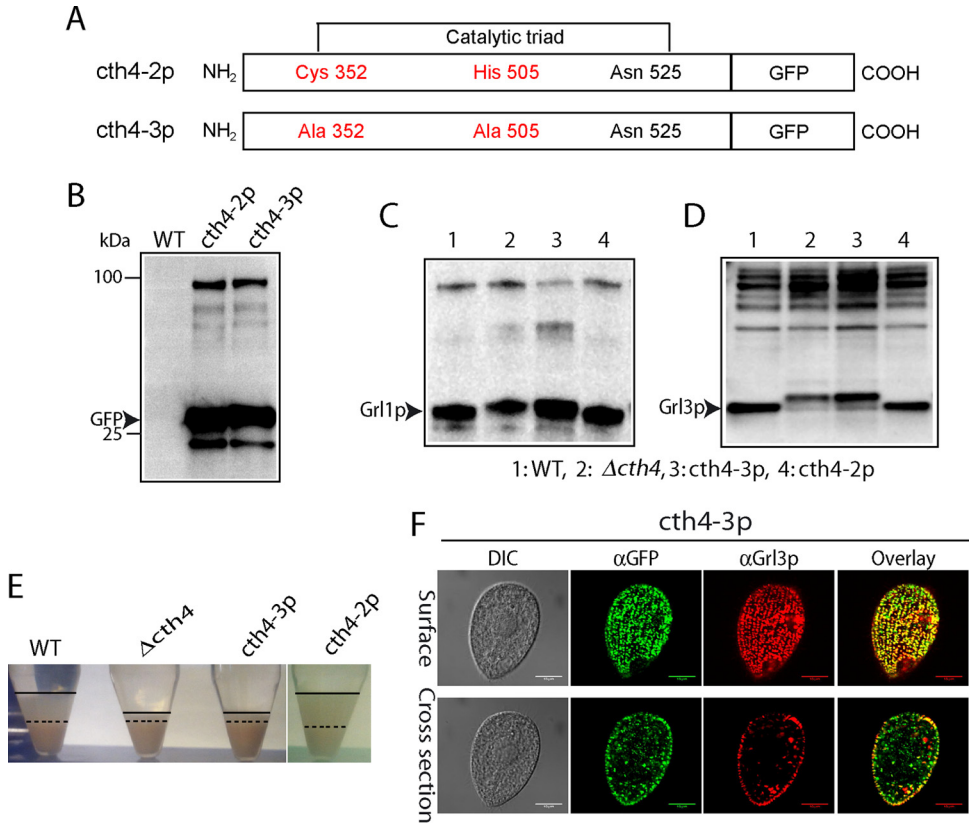

FIG 10 *CTH4* activity requires conserved active site residues. (A) Schematic of wild-type and mutant Cth4p, both with C-terminal GFP tags, showing locations of mutations (Cys^{352}→Ala and His^{505}→Ala) within the conserved catalytic triad. (B) Expression of GFP-tagged and mutant Cys^{352}→Ala and His^{505}→Ala constructs (*cth4-2* and *cth4-3*, respectively). Constructs were expressed at the *CTH4* locus, via gene replacement. Fusion proteins were immunoprecipitated from detergent lysates using rabbit anti-GFP antiserum, transferred to PVDF, and probed with MAb anti-GFP. The transformed cell lines show immunoreactive bands of the size expected for the Cth4p-GFP fusions, as well as a band likely to correspond to monomeric GFP. (C and D) proGrl processing in wild-type and mutant cell lines. Cell lysates (5×10^3 cell equivalents in panel C and 10^4 cell equivalents in panel D) were separated by SDS-PAGE and probed with anti-Grl1p antibody. Wild-type and *cth4-2* cells accumulate mature Grl1p. In contrast, Δ*cth4* cells and *cth4-3* cells accumulate proGrl1p and a species slightly larger than mature wild-type Grl1p. (D) Same as panel C, but with blotting with anti-Grl3p antibody. (E) Dibucaine stimulation of cell lines in panels C and D. Wild-type cells and cells expressing cth4-2p generate large flocculent layers (between the solid and broken lines), while Δ*cth4* and cells expressing cth4-3p show a smaller amount of flocculent. (F) Cells expressing cth4-3p were fixed, permeabilized, and immunostained for GFP and for Grl3p. Localization of the mutated cth4-3p is similar to that of the wild-type enzyme, in both cytoplasmic puncta and docked mucocysts. Scale bars = 10 μm.

was C-terminally tagged with 6×His, with the idea that a small epitope tag might be less subject to removal by cytosolic proteases than a globular protein tag like GFP. Indeed, we found that His-tagged Cth4p, expressed in wild-type cells, accumulated as three major bands in growing cells (Fig. 12, lane 2). These could tentatively be assigned to three different processed forms of Cth4p, although the precise junctions between domains in the *Tetrahymena* protein cannot be predicted due to the relatively low sequence conservation in those regions (Fig. 12B). The same three bands were present in Δ*cth3* lysates, though there were relatively lower levels of the HL species than of the wild type.

The apparent difference in the processing of Cth4p-6×His in Δ*cth3* cells was more striking when cultures were sampled during starvation. Importantly, starvation is known to accelerate proGrl processing and also induce expression of both *CTH3* and *CTH4* (Fig. 1A) (45). Starved wild-type cells showed accumulation of the EIHL and HL species (see Fig. 12A), the latter predicted to represent the active enzyme. In contrast, in starved Δ*cth3* cells virtually all cth4p-6×His accumulated as the unprocessed EIHL species, which is predicted to be inactive. These results suggest that Cth3p activity is involved, directly or indirectly, in proteolytic activation of Cth4p zymogen.

DISCUSSION

The proteinaceous cores of secretory granule-like organelles in oligohymenophorean ciliates, best studied for *Tetrahymena thermophila* and *Paramecium tetraurelia*, are remarkable structures that assemble as complex multicomponent crystals and then are transformed into projectiles during exocytosis, by undergoing rapid ordered expansion. Pioneering studies in the 1980s established that the proteolytic processing of proproteins was likely to be a key mechanism in controlling core assembly, and this was substantiated by subsequent identification and analysis of the protein-encoding genes as well as detailed characterization of the secreted polypeptides (24–26, 50). Nonetheless, the proteases themselves could only be inferred until recently, when expression profiling led to an aspartyl cathepsin, Cth3p (27). The failure of Δ*cth3* cells to process *Tetrahymena* mucocyst proproteins and to assemble ordered mucocysts provided strong direct confirmation that proteases were key determinants in this pathway. In the cur-

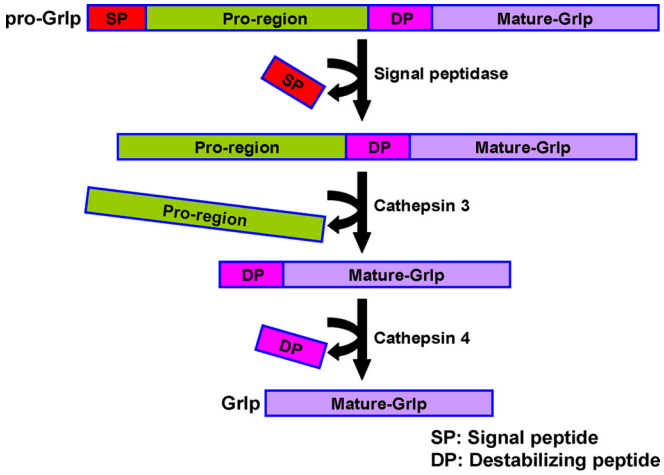

FIG 11 Model for proteolytic processing of mucocyst proGrl proteins in *Tetrahymena*. We propose that processing of proGrl proteins during mucocyst maturation initiates with endoproteolytic cleavage by Cth3p at a site upstream of the mature N termini. The products are competent to form highly ordered complexes that assemble to create the elongated mucocyst core. Cth4p subsequently acts to trim the amino termini. This step is proposed to be essential for reinforcing the lattice in a way that promotes stability during expansion. Since removal of the peptides results in stabilization during expansion, we have termed them "destabilizing peptides" (DP). The relative timing of DP removal versus assembly is unknown. Cores that have not undergone DP trimming are defective during the directional expansion required for efficient core extrusion during exocytosis.

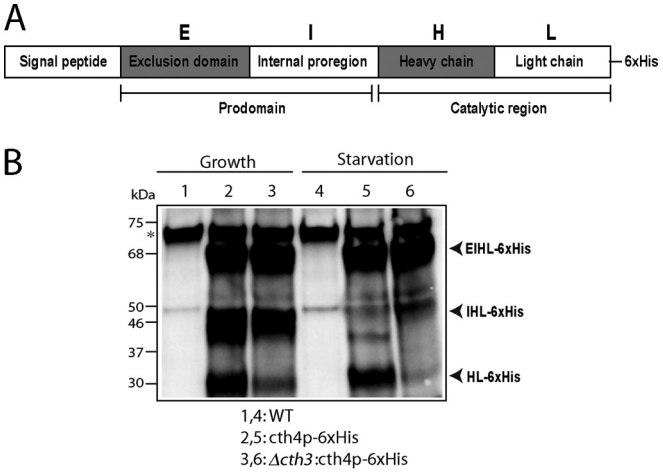

FIG 12 Cth4p undergoes Cth3p-dependent processing (A) Proposed organization of *T. thermophila* Cth4p, based on established structures of cathepsin C homologs in other eukaryotes. S, signal sequence; E, exclusion prodomain; I, internal proregion; H, heavy chain; L, light chain. The catalytic domains are the heavy and light chains. (B) Processed forms of Cth4p in *T. thermophila*. Cth4p-6×His expression was induced for 2 h in wild-type or Δ*cth3* cultures. Cells were induced in either growth or starvation media, by adding 1 or 0.1 μg/ml of $CdCl_2$, respectively. Cell lysates (3×10^4 cell equivalents/lane) were separated by SDS-PAGE and Western blots were probed with anti-His MAb. Three major His-tagged species are present, and their tentative relationship with the domains indicated in panel A is indicated. Particularly in starvation, the large majority of Cth4p in Δ*cth3* cells remains in an unprocessed form that is predicted to be inactive. Note that starvation is a state in which transcription of Cth3p and Cth4p, as well as processing of proGrl, are induced.

rent study, we used expression profiling to focus on a second protease that is required in the formation of functional mucocysts. *CTH4* belongs to a family of papain-related enzymes of the cathepsin C subfamily, with cysteine at the active site, and is therefore only distantly related to *CTH3*.

CTH4 is important for mucocyst function. This is easily demonstrated using a secretion assay in which wild-type mucocyst cores, following their exocytic expansion and extrusion, are pelleted to create a measurable flocculent layer. Δ*cth4* cells showed a dramatic decrease in flocculent formation, which reflects several defects that are likely to be mechanistically related. First, Δ*cth4* cells stimulated to undergo mucocyst exocytosis release only a fraction of the protein released by wild-type cells, which we gauged by immunolabeling and flow cytometry to be ~50%. The stimulated Δ*cth4* cells also show limited expansion of the mucocyst cores, as revealed by electron microscopy: whereas wild-type mucocyst cores are completely extruded during exocytosis, many Δ*cth4* cores are retained after stimulation within docked mucocyst remnants. In wild-type cells, mucocyst core expansion appears to involve calcium binding to multiple low-affinity sites on the Grl proteins, resulting in irreversible crystalline expansion (20). The crystals themselves, based on analysis of the homologous organelles in *Paramecium*, may be organized as bundles of fibrils, but the molecular rearrangements that occur during expansion are unknown (21, 51). In Δ*cth4* cells, the poststimulation cores appear wider than those in resting cells, as well as disordered with no visible lattice structure. A simple idea is that aberrant expansion of Δ*cth4* cores leads to their incomplete extrusion and therefore inefficient protein secretion. This limited extrusion may be due to lattice disassembly during expansion, as suggested by fractionation experiments on secreted mucocyst cores. The protein released by Δ*cth4* cells shows far less of a tendency to form a flocculent layer and instead remains soluble. The aggregates released from Δ*cth4* cells are therefore smaller and/or less stable than those in the wild type, suggesting that protein-protein interactions within the Grl-based crystals that are formed in the absence of Cth4p are weaker or less extensive than in the wild type.

The Δ*cth4* phenotype recalls a single mutant in *Paramecium caudatum*, called tnd1 (52). The secretory granule cores in tnd1 cells fail to expand and therefore extrude upon stimulation, and this was correlated with an apparent defect in proprotein processing in the core proteins. However, the genetic lesion in the tnd1 mutant is as yet unknown.

At the biochemical level, analysis of Δ*cth4* cells revealed novel features of mucocyst assembly. The processed Grl polypeptides in Δ*cth4* cells retain short N-terminal extensions, revealing probable transient biochemical intermediates not detected in prior studies. One implication is that the initial endoproteolytic cleavage of the proGrl precursors must occur at sites upstream of those proposed in current models (20, 53). Since *CTH4* has clear orthologs in *P. tetraurelia*, we assume that similar exoproteolytic trimming is responsible for generating the mature amino termini in this ciliate as well (54). A second defect in Δ*cth4* cells is the presence of fully unprocessed proGrl proteins that accumulate in docked mucocysts and could be released upon dibucaine stimulation. Since proGrl processing is the driver of lattice assembly, the presence of unprocessed proGrl proteins may destabilize the cores in Δ*cth4* cells. However, although we clearly detected higher levels of proGrl precursors in Δ*cth4* mucocysts, the true ratio of Grl precursors to products is likely to be much lower than it appears by Western blotting, since the Grl proproteins show much higher immunore-

activity than the mature forms on Western blots (unpublished data). For this reason, we instead propose that destabilization of the cores chiefly results from the uniformly untrimmed amino-terminal peptides in the mature Grl polypeptides. These additional peptides are unlikely to interfere with proper folding, since the Grl products still assemble into visible lattices, and we did not detect any morphologically aberrant mucocysts in Δ*cth4* samples. However, amino-terminal trimming may be required to permit additional interactions that are required to maintain the integrity of the lattice, especially during expansion. Carboxy-terminal trimming of Grl products is also likely to occur during mucocyst biogenesis, judging by the identification of a carboxypeptidase, Car1p, which localizes to mucocysts (27; unpublished data). However, disruption of *CAR1* did not produce a secretion phenotype, so such trimming may serve a nonstructural purpose (unpublished data).

In wild-type cells, the amino-terminal extensions must be removed by endoproteolytic cleavage and/or exoproteolytic trimming, and this may be accomplished directly by Cth4p. Cells expressing a variant of *CTH4*, in which the conserved catalytic residues were mutated, were phenotypically equivalent to Δ*cth4* cells, which strongly suggests that all *in vivo* functions of Cth4p rely on its predicted enzymatic activity. In other organisms, proteins in the cathepsin C subfamily demonstrate both endoproteolytic and exoproteolytic activities, depending on the enzyme oligomerization state (55). Among cathepsin C family members whose activities have been characterized, the one most closely related to Cth4p is an enzyme from *T. gondii* (TgCPC2, annotated as Tg6 in Fig. 1B) (48). *T. gondii* is an apicomplexan and therefore belongs to a sister group of the ciliates (56). This enzyme showed exoproteolytic activity *in vitro*, but endoproteolytic activity was not examined.

The simplest model consistent with our data is that Cth3p and Cth4p act sequentially on the same substrates. Cth3p is required for the primary endoproteolytic cleavage of Grl proproteins, and Cth4p acts on products of that cleavage. However, our data do not rule out the possibility that Cth3p and/or Cth4p also has important non-Grl substrates. In addition, the current data do not distinguish between Cth4p acting directly upon proGrl substrates or being indirectly responsible for processing, e.g., by activating another enzyme which directly acts upon proGrls. In *T. gondii*, a cathepsin L enzyme, TgCPL, processes dissimilar substrates that are moreover targeted to two different compartments: secretory organelles (micronemes) and an acidic compartment termed the plant-like vacuole (PLV) (57, 58).

Cathepsin C family members were initially considered lysosomal hydrolases, and the role of Cth4p in mucocyst biogenesis is therefore consistent with the idea that secretory organelles in ciliates are related to lysosome-related organelles and underscores the idea that adapting the machinery of lysosome biogenesis has been a major evolutionary mechanism driving organellar diversity in different tissues and lineages (39) (16, 59, 60). Interestingly, the functions provided by cathepsin C members in animals extend beyond proteolytic degradation of lysosome contents. In particular, the aminopeptidase activity can activate serine proteases by removing inhibitory short amino-terminal peptides (61). Proteolytic activation by cysteine proteases also occurs in *T. gondii* (58). Thus, the defects in Δ*cth4* cells may reflect the failure to activate additional enzymes, rather than the direct action of Cth4p on Grl proproteins. Our survey of protease genes in *T. thermophila* revealed five that are coregulated with the *GRL* genes, and all are targeted to mucocysts (27; unpublished data). However, we disrupted each of these genes, and only *CTH3* resulted in a secretion phenotype ofa severity comparable to that of *CTH4* (unpublished data). However, as noted above, Cth4p cannot be required for activation of Cth3p since Δ*cth3* manifests the more severe exocytosis deficiency. Therefore, if Cth4p acts primarily by activating a second processing enzyme, that protein is likely to be novel. Whether or not Cth4p acts on downstream enzymes, our data suggest that it is itself activated by Cth3p under starvation conditions, while other functionally overlapping cathepsins encoded by this large gene family may be more relevant during growth conditions.

Cth4p acts during mucocyst maturation, and the simplest hypothesis is that it functions in an immature mucocyst compartment, for which we are currently developing molecular markers. Cth4p, like Cth3p, showed significant overlap in localization studies with endolysosomal markers. Whether the immature mucocyst compartment is itself labeled with FM4-64, i.e., whether it receives vesicular traffic from endosomes, is not known. One interesting possibility is that Cth4p may not be directly transported from the TGN to immature mucocysts, since we detected numerous cytoplasmic puncta that are positive for Cth4p-GFP but not Grl3p in cells that have been induced for short times to express the tagged gene. A related question is whether Cth3p and Cth4p are active in the same compartment. One notable difference between the two is that Cth3p, but not Cth4p, was readily detected in cell culture supernatants, suggesting that only the former accumulates in a compartment that releases its contents to the cell medium (27). In the future, these issues may be clarified by determining the targeting mechanisms used for the different proteases.

Endoproteolyic cleavage followed by obligatory trimming is a feature of many proproteins packaged in animal secretory granules, such as proinsulin (3). The similarity with proprotein processing in secretory organelles in ciliates, as revealed by analysis of Cth3p and Cth4p, offers a striking example of convergent solutions, based on evolutionarily unrelated enzymes, to the problem of generating and packaging bioactive peptides.

ACKNOWLEDGMENTS

This research was supported by NSF grant MCB-1051985 and NIH grant GM105783 to A.P.T.

We thank Vytas Bindokas and Christine Labno (University of Chicago Light Microscopy Core Facility) for help with light microscopy, Yimei Chen (University of Chicago EM Core Facility) for electron microscopy, Don Wolfgeher (University of Chicago Mass Spectrometry Core Facility), and Dhaval Nanavati (Northwestern University Mass Spectrometry Core Facility). Doug Chalker (Washington University, MO) generously shared *Tetrahymena*-specific tagging vectors, and E. Marlo Nelsen and Joseph Frankel (University of Iowa) generously provided MAbs 4D11 and 5E9.

A.P.T. serves on the scientific advisory board of Tetragenetics, Inc.

REFERENCES

1. **Albrethsen J, Goetze JP, Johnsen AH.** 2015. Mining the granule proteome: a potential source of endocrine biomarkers. Biomark Med **9:**259–265. http://dx.doi.org/10.2217/bmm.14.107.
2. **Meldolesi J, Chieregatti E, Luisa Malosio M.** 2004. Requirements for the identification of dense-core granules. Trends Cell Biol **14:**13–19. http://dx.doi.org/10.1016/j.tcb.2003.11.006.
3. **Steiner DF.** 2011. On the discovery of precursor processing. Methods Mol Biol **768:**3–11.
4. **Orci L, Ravazzola M, Amherdt M, Madsen O, Vassalli JD, Perrelet A.** 1985.

Direct identification of prohormone conversion site in insulin-secreting cells. Cell **42:**671–681. http://dx.doi.org/10.1016/0092-8674(85)90124-2.
5. **Arvan P, Castle D.** 1998. Sorting and storage during secretory granule biogenesis: looking backward and looking forward. Biochem J **332:**593–610.
6. **Morvan J, Tooze SA.** 2008. Discovery and progress in our understanding of the regulated secretory pathway in neuroendocrine cells. Histochem Cell Biol **129:**243–252. http://dx.doi.org/10.1007/s00418-008-0377-z.
7. **Steiner DF.** 1998. The proprotein convertases. Curr Opin Chem Biol **2:**31–39. http://dx.doi.org/10.1016/S1367-5931(98)80033-1.
8. **Fricker LD.** 1988. Carboxypeptidase E. Annu Rev Physiol **50:**309–321. http://dx.doi.org/10.1146/annurev.ph.50.030188.001521.
9. **Naggert JK, Fricker LD, Varlamov O, Nishina PM, Rouille Y, Steiner DF, Carroll RJ, Paigen BJ, Leiter EH.** 1995. Hyperproinsulinaemia in obese fat/fat mice associated with a carboxypeptidase E mutation which reduces enzyme activity. Nat Genet **10:**135–142. http://dx.doi.org/10.1038/ng0695-135.
10. **Steiner DF, Rouille Y, Gong Q, Martin S, Carroll R, Chan SJ.** 1996. The role of prohormone convertases in insulin biosynthesis: evidence for inherited defects in their action in man and experimental animals. Diabetes Metab **22:**94–104.
11. **Arkowitz RA.** 2009. Chemical gradients and chemotropism in yeast. Cold Spring Harbor Perspect Biol **1:**a001958.
12. **Loomis WF.** 2014. Cell signaling during development of Dictyostelium. Dev Biol **391:**1–16. http://dx.doi.org/10.1016/j.ydbio.2014.04.001.
13. **Gallagher KL, Sozzani R, Lee CM.** 2014. Intercellular protein movement: deciphering the language of development. Annu Rev Cell Dev Biol **30:**207–233. http://dx.doi.org/10.1146/annurev-cellbio-100913-012915.
14. **Turkewitz AP.** 2004. Out with a bang! Tetrahymena as a model system to study secretory granule biogenesis. Traffic **5:**63–68. http://dx.doi.org/10.1046/j.1600-0854.2003.00155.x.
15. **Vayssié L, Skouri F, Sperling L, Cohen J.** 2000. Molecular genetics of regulated secretion in Paramecium. Biochimie **82:**269–288. http://dx.doi.org/10.1016/S0300-9084(00)00201-7.
16. **Briguglio JS, Kumar S, Turkewitz AP.** 2013. Lysosomal sorting receptors are essential for secretory granule biogenesis in Tetrahymena. J Cell Biol **203:**537–550. http://dx.doi.org/10.1083/jcb.201305086.
17. **Tokuyasu K, Scherbaum OH.** 1965. Ultrastructure of mucocysts and pellicle of Tetrahymena pyriformis. J Cell Biol **27:**67–81. http://dx.doi.org/10.1083/jcb.27.1.67.
18. **Plattner H.** 2015. Molecular aspects of calcium signalling at the crossroads of unikont and bikont eukaryote evolution—the ciliated protozoan Paramecium in focus. Cell Calcium **57:**174–185. http://dx.doi.org/10.1016/j.ceca.2014.12.002.
19. **Satir BH, Schooley C, Satir P.** 1973. Membrane fusion in a model system. Mucocyst secretion in Tetrahymena. J Cell Biol **56:**153–176.
20. **Verbsky JW, Turkewitz AP.** 1998. Proteolytic processing and Ca2+-binding activity of dense-core vesicle polypeptides in Tetrahymena. Mol Biol Cell **9:**497–511. http://dx.doi.org/10.1091/mbc.9.2.497.
21. **Sperling L, Tardieu A, Gulik-Krzywicki T.** 1987. The crystal lattice of Paramecium trichocysts before and after exocytosis by X-ray diffraction and freeze-fracture electron microscopy. J Cell Biol **105:**1649–1662. http://dx.doi.org/10.1083/jcb.105.4.1649.
22. **Cowan AT, Bowman GR, Edwards KF, Emerson JJ, Turkewitz AP.** 2005. Genetic, genomic, and functional analysis of the granule lattice proteins in Tetrahymena secretory granules. Mol Biol Cell **16:**4046–4060. http://dx.doi.org/10.1091/mbc.E05-01-0028.
23. **Bowman GR, Smith DG, Michael Siu KW, Pearlman RE, Turkewitz AP.** 2005. Genomic and proteomic evidence for a second family of dense core granule cargo proteins in Tetrahymena thermophila. J Eukaryot Microbiol **52:**291–297. http://dx.doi.org/10.1111/j.1550-7408.2005.00045.x.
24. **Madeddu L, Gautier MC, Le Caer JP, Garreau de Loubresse N, Sperling L.** 1994. Protein processing and morphogenesis of secretory granules in Paramecium. Biochimie **76:**329–335. http://dx.doi.org/10.1016/0300-9084(94)90167-8.
25. **Collins T, Wilhelm JM.** 1981. Post-translational cleavage of mucocyst precursors in Tetrahymena. J Biol Chem **256:**10475–10484.
26. **Adoutte A, Garreau de Loubresse N, Beisson J.** 1984. Proteolytic cleavage and maturation of the crystalline secretion products of Paramecium. J Mol Biol **180:**1065–1081. http://dx.doi.org/10.1016/0022-2836(84)90271-7.
27. **Kumar S, Briguglio JS, Turkewitz AP.** 2014. An aspartyl cathepsin, CTH3, is essential for proprotein processing during secretory granule maturation in Tetrahymena thermophila. Mol Biol Cell **25:**2444–2460. http://dx.doi.org/10.1091/mbc.E14-03-0833.
28. **Miao W, Xiong J, Bowen J, Wang W, Liu Y, Braguinets O, Grigull J, Pearlman RE, Orias E, Gorovsky MA.** 2009. Microarray analyses of gene expression during the Tetrahymena thermophila life cycle. PLoS One **4:**e4429. http://dx.doi.org/10.1371/journal.pone.0004429.
29. **Xiong J, Lu X, Zhou Z, Chang Y, Yuan D, Tian M, Wang L, Fu C, Orias E, Miao W.** 2012. Transcriptome analysis of the model protozoan, Tetrahymena thermophila, using deep RNA sequencing. PLoS One **7:**e30630. http://dx.doi.org/10.1371/journal.pone.0030630.
30. **Xiong J, Lu Y, Feng J, Yuan D, Tian M, Chang Y, Fu C, Wang G, Zeng H, Miao W.** 2013. Tetrahymena functional genomics database (TetraFGD): an integrated resource for Tetrahymena functional genomics. Database (Oxford) **2013:**bat008.
31. **Stover NA, Punia RS, Bowen MS, Dolins SB, Clark TG.** 2012. Tetrahymena Genome Database Wiki: a community-maintained model organism database. Database (Oxford) **2012:**bas007.
32. **Coyne RS, Thiagarajan M, Jones KM, Wortman JR, Tallon LJ, Haas BJ, Cassidy-Hanley DM, Wiley EA, Smith JJ, Collins K, Lee SR, Couvillion MT, Liu Y, Garg J, Pearlman RE, Hamilton EP, Orias E, Eisen JA, Methe BA.** 2008. Refined annotation and assembly of the Tetrahymena thermophila genome sequence through EST analysis, comparative genomic hybridization, and targeted gap closure. BMC Genomics **9:**562. http://dx.doi.org/10.1186/1471-2164-9-562.
33. **Cassidy-Hanley D, Bowen J, Lee JH, Cole E, VerPlank LA, Gaertig J, Gorovsky MA, Bruns PJ.** 1997. Germline and somatic transformation of mating Tetrahymena thermophila by particle bombardment. Genetics **146:**135–147.
34. **Rahaman A, Miao W, Turkewitz AP.** 2009. Independent transport and sorting of functionally distinct protein families in Tetrahymena dense core secretory granules. Eukaryot Cell **8:**1575–1583. http://dx.doi.org/10.1128/EC.00151-09.
35. **Kumar S, Sheokand N, Mhadeshwar MA, Raje CI, Raje M.** 2012. Characterization of glyceraldehyde-3-phosphate dehydrogenase as a novel transferrin receptor. Int J Biochem Cell Biol **44:**189–199. http://dx.doi.org/10.1016/j.biocel.2011.10.016.
36. **Keller A, Nesvizhskii AI, Kolker E, Aebersold R.** 2002. Empirical statistical model to estimate the accuracy of peptide identifications made by MS/MS and database search. Anal Chem **74:**5383–5392. http://dx.doi.org/10.1021/ac025747h.
37. **Nesvizhskii AI, Keller A, Kolker E, Aebersold R.** 2003. A statistical model for identifying proteins by tandem mass spectrometry. Anal Chem **75:**4646–4658. http://dx.doi.org/10.1021/ac0341261.
38. **Shang Y, Song X, Bowen J, Corstanje R, Gao Y, Gaertig J, Gorovsky MA.** 2002. A robust inducible-repressible promoter greatly facilitates gene knockouts, conditional expression, and overexpression of homologous and heterologous genes in Tetrahymena thermophila. Proc Natl Acad Sci U S A **99:**3734–3739. http://dx.doi.org/10.1073/pnas.052016199.
39. **Lecaille F, Kaleta J, Bromme D.** 2002. Human and parasitic papain-like cysteine proteases: their role in physiology and pathology and recent developments in inhibitor design. Chem Rev **102:**4459–4488. http://dx.doi.org/10.1021/cr0101656.
40. **Elde NC, Morgan G, Winey M, Sperling L, Turkewitz AP.** 2005. Elucidation of clathrin-mediated endocytosis in tetrahymena reveals an evolutionarily convergent recruitment of dynamin. PLoS Genet **1:**e52. http://dx.doi.org/10.1371/journal.pgen.0010052.
41. **Satir B.** 1977. Dibucaine-induced synchronous mucocyst secretion in Tetrahymena. Cell Biol Int Rep **1:**69–73. http://dx.doi.org/10.1016/0309-1651(77)90012-1.
42. **Tiedtke A.** 1976. Capsule shedding in Tetrahymena. Naturwissenschaften **63:**93. http://dx.doi.org/10.1007/BF00622415.
43. **Turkewitz AP, Kelly RB.** 1992. Immunocytochemical analysis of secretion mutants of Tetrahymena using a mucocyst-specific monoclonal antibody. Dev Genet **13:**151–159. http://dx.doi.org/10.1002/dvg.1020130209.
44. **Maihle NJ, Satir BH.** 1986. Protein secretion in Tetrahymena thermophila. Characterization of the major proteinaceous secretory proteins. J Biol Chem **261:**7566–7570.
45. **Turkewitz AP, Madeddu L, Kelly RB.** 1991. Maturation of dense core granules in wild type and mutant Tetrahymena thermophila. EMBO J **10:**1979–1987.
46. **Melia SM, Cole ES, Turkewitz AP.** 1998. Mutational analysis of regulated exocytosis in Tetrahymena. J Cell Sci **111:**131–140.
47. **Hooper NM.** 2002. Proteases: a primer. Essays Biochem **38:**1–8.
48. **Que X, Engel JC, Ferguson D, Wunderlich A, Tomavo S, Reed SL.** 2007. Cathepsin Cs are key for the intracellular survival of the protozoan para-

site, Toxoplasma gondii. J Biol Chem **282:**4994–5003. http://dx.doi.org/10.1074/jbc.M606764200.

49. **Yang W, Xia W, Mao J, Xu D, Chen J, Feng S, Wang J, Li H, Theisen CF, Petersen JM, Thorolfsson M, Rasmussen HB, Junker F, Boel E, Su J.** 2011. High level expression, purification and activation of human dipeptidyl peptidase I from mammalian cells. Protein Expr Purif **76:**59–64. http://dx.doi.org/10.1016/j.pep.2010.09.001.
50. **Chilcoat ND, Melia SM, Haddad A, Turkewitz AP.** 1996. Granule lattice protein 1 (Grl1p), an acidic, calcium-binding protein in Tetrahymena thermophila dense-core secretory granules, influences granule size, shape, content organization, and release but not protein sorting or condensation. J Cell Biol **135:**1775–1787. http://dx.doi.org/10.1083/jcb.135.6.1775.
51. **Peterson JB, Heuser JE, Nelson DL.** 1987. Dissociation and reassociation of trichocyst proteins: biochemical and ultrastructural studies. J Cell Sci **87:**3–25.
52. **Klauke N, Kissmehl R, Plattner H, Haga N, Watanabe T.** 1998. An exocytotic mutant of Paramecium caudatum: membrane fusion without secretory contents release. Cell Calcium **23:**349–360. http://dx.doi.org/10.1016/S0143-4160(98)90030-6.
53. **Bradshaw NR, Chilcoat ND, Verbsky JW, Turkewitz AP.** 2003. Proprotein processing within secretory dense core granules of Tetrahymena thermophila. J Biol Chem **278:**4087–4095. http://dx.doi.org/10.1074/jbc.M207236200.
54. **Vayssié L, Garreau De Loubresse N, Sperling L.** 2001. Growth and form of secretory granules involves stepwise assembly but not differential sorting of a family of secretory proteins in Paramecium. J Cell Sci **114:**875–886.
55. **Turk D, Janjic V, Stern I, Podobnik M, Lamba D, Dahl SW, Lauritzen C, Pedersen J, Turk V, Turk B.** 2001. Structure of human dipeptidyl peptidase I (cathepsin C): exclusion domain added to an endopeptidase framework creates the machine for activation of granular serine proteases. EMBO J **20:**6570–6582. http://dx.doi.org/10.1093/emboj/20.23.6570.
56. **Parfrey LW, Barbero E, Lasser E, Dunthorn M, Bhattacharya D, Patterson DJ, Katz LA.** 2006. Evaluating support for the current classification of eukaryotic diversity. PLoS Genet **2:**e220. http://dx.doi.org/10.1371/journal.pgen.0020220.
57. **Dou Z, Carruthers VB.** 2011. Cathepsin proteases in Toxoplasma gondii. Adv Exp Med Biol **712:**49–61.
58. **Dou Z, Coppens I, Carruthers VB.** 2013. Non-canonical maturation of two papain-family proteases in Toxoplasma gondii. J Biol Chem **288:**3523–3534. http://dx.doi.org/10.1074/jbc.M112.443697.
59. **Elde NC, Long M, Turkewitz AP.** 2007. A role for convergent evolution in the secretory life of cells. Trends Cell Biol **17:**157–164. http://dx.doi.org/10.1016/j.tcb.2007.02.007.
60. **Raposo G, Marks MS, Cutler DF.** 2007. Lysosome-related organelles: driving post-Golgi compartments into specialisation. Curr Opin Cell Biol **19:**394–401. http://dx.doi.org/10.1016/j.ceb.2007.05.001.
61. **Pham CT, Ley TJ.** 1999. Dipeptidyl peptidase I is required for the processing and activation of granzymes A and B in vivo. Proc Natl Acad Sci U S A **96:**8627–8632. http://dx.doi.org/10.1073/pnas.96.15.8627.